

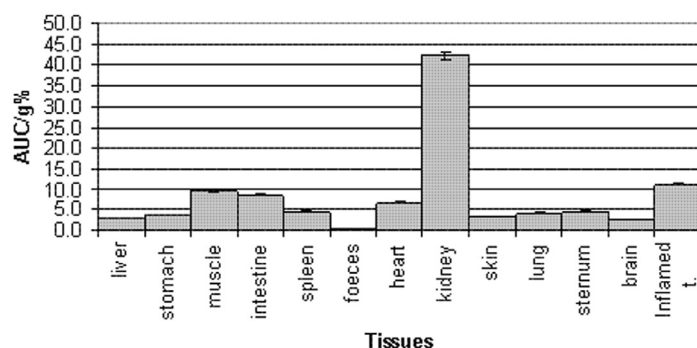
P295 EVALUATION OF (^{201}Tl)(III)-DTPA-HiGg FOR INFLAMMATION DETECTION IN RATSA. KHORRAMI¹, A.R. JALILIAN², M.B. TAVAKOLI¹, M. KAMALI-DEGHAN², Y. YARI KAMRANI² and S. MORADKHANI²¹Medical Physics and Engineering Department, Medical Sciences University of Isfahan, Isfahan, Islamic Republic of Iran; ²Cyclotron and Nuclear Medicine Department, Nuclear Research Center for Agriculture and Medicine, Karaj, Tehran, Islamic Republic of Iran

Introduction: Thallium-201 ($T_{1/2}=3.04$ d) in Tl^+ form was converted to Tl^{3+} cation in presence of O_3 in 6M HCl controlled by RTLC/gel electrophoresis methods and used in the labeling of human polyclonal antibody (HiGg) after resolidation with freshly prepared cyclic DTPA-dianhydride.

Experimental: The best results of the conjugation were obtained by the addition of 1 ml of a HiGg pharmaceutical solution (5 mg/ml, in phosphate buffer, pH=7) to a glass tube pre-coated with DTPA-dianhydride (0.01 mg) at 25°C with continuous mild stirring for 30 min. The final isotonic [^{201}Tl](III)-DTPA-HiGg complex was checked by radio-TLC using several solvent systems to ensure the formation of only one species followed by filtration through a 0.22 μ filter (specific activity = 33.7 TBq/mM, radiochemical purity > 95%).

Chemical species	Mobile phase	Stationary phase	R_f
^{201}Tl -DTPA-HiGg	10% ammonium acetate:methanol (1:1)	silicagel	0.3
$^{201}\text{Tl}^{3+}$	10% ammonium acetate:methanol (1:1)	silicagel	0.2
^{201}Tl -DTPA	10% ammonium acetate:methanol (1:1)	silicagel	0.7
^{201}Tl -DTPA-HiGg	0.9% sodium chloride solution	silicagel	0.2
$^{201}\text{Tl}^{3+}$	0.9% sodium chloride solution	silicagel	0.0
^{201}Tl -DTPA	0.9% sodium chloride solution	silicagel	0.5
^{201}Tl -DTPA-HiGg	pyridine:ethanol:water (1:2:4)	silicagel	0.0
$^{201}\text{Tl}^{3+}$	pyridine:ethanol:water (1:2:4)	silicagel	0.1
^{201}Tl -DTPA	pyridine:ethanol:water (1:2:4)	silicagel	0.7
^{201}Tl -DTPA-HiGg	water:methanol (45:55)	Paper chromatography, Whatman No. 1	0.2
$^{201}\text{Tl}^{3+}$	water:methanol (45:55)	Paper chromatography, Whatman No. 1	0.1
^{201}Tl -DTPA	water:methanol (45:55)	Paper chromatography, Whatman No. 1	0.8
^{201}Tl -DTPA-HiGg	1 mM DTPA	Paper chromatography, Whatman No. 1	0.4
$^{201}\text{Tl}^{3+}$	1 mM DTPA	Paper chromatography, Whatman No. 1	0.9
^{201}Tl -DTPA	1 mM DTPA	Paper chromatography, Whatman No. 1	0.6
^{201}Tl -DTPA-HiGg	1 mM DTPA	silicagel	0.0
$^{201}\text{Tl}^{3+}$	1 mM DTPA	silicagel	0.0
^{201}Tl -DTPA	1 mM DTPA	silicagel	0.8

Results and Discussion: Preliminary bio-distribution studies in normal and inflammation-bearing rats were performed. The target/skin and target/blood ratios were 4 and 6 after 28h respectively, showing the selectivity of the radiopharmaceutical for the inflammatory lesions.



Conclusion: [^{201}Tl](III)-DTPA-HiGg showed to possess interesting inflammation-seeking properties in turpentine-oil treated rats. the biological activity of the complex must be checked in other inflammation models.

Keywords: ^{201}Tl (III)-Complex, Biodistribution, Human Polyclonal Antibody, Inflammation

P296 [¹¹C]ROFECOXIB AS PET TRACER FOR COX-2: EVALUATION IN A HSV ENCEPHALITIS MODEL**E.F.J. DE VRIES, J. DOORDUIN, A. VAN WAARDE and R.A. DIERCKX**

Nuclear Medicine and Molecular Imaging, University Medical Center Groningen, University of Groningen, Groningen, Netherlands

Introduction: Cyclooxygenase-2 (COX-2), a key enzyme in prostaglandin biosynthesis, is induced during inflammation. Overexpression of COX-2 is thought to have a detrimental effect in disorders like inflammation, neurodegeneration and cancer. In our previous work, we have evaluated [¹¹C]rofecoxib as a PET tracer for COX-2. Although brain uptake of [¹¹C]rofecoxib in healthy rats corresponded with COX-2 distribution and some specific binding (20-40% of total uptake) was observed, the results were inconclusive, because of the low basal expression of COX-2. In this study, we investigated if inflammation-induced COX-2 overexpression in viral encephalitis could be detected with [¹¹C]rofecoxib PET.

Experimental: At day 0, viral encephalitis was induced in male Wistar rats by intranasal application of 10⁷ pfu herpes simplex virus type 1 in 100 µl PBS (n=5). Controls were treated identically using PBS without virus (n=7). After intranasal infection, the replicating virus migrates into the brain where it induces substantial inflammation that causes visible symptoms of illness from day 5 on. At day 6 or 7, the rats were anaesthetized and i.v. injected with 54±4 MBq [¹¹C]rofecoxib. A dynamic PET scan (microPET Focus 220) was acquired for 60 min, followed by ex vivo biodistribution. In blocking experiments, the non-selective COX inhibitor indomethacin (2.5 mg/kg) was i.v. injected 5 min before injection of the tracer (n=4).

Results and Discussion: For all experimental groups, [¹¹C]rofecoxib PET images of the brain showed low tracer uptake at 60 min with minor regional differences. After the initial distribution phase, clearance of the tracer from the brain was slow (T_{1/2} >60 min). Ex vivo biodistribution in healthy controls showed highest [¹¹C]rofecoxib brain uptake in structures with highest basal COX-2 expression: cingulate/frontopolar cortex (SUV 0.35±0.11) and hippocampus (SUV 0.30±0.11). Compared to healthy controls, infected animals showed a moderate increase (5-58%) in tracer uptake in all brain regions, but this increase was not statistically significant for any region (p>0.14). The increase in [¹¹C]rofecoxib uptake did not correspond with the distribution of microglia activation, as was determined by [¹¹C]PK11195 PET in a parallel study. At 60 min, radioactivity in plasma was significantly higher in infected animals than in controls (SUV 0.54±0.20 vs. 0.83±0.14, p=0.02), which could explain the elevated brain uptake. Administration of indomethacin to the infected animals did not significantly reduce [¹¹C]rofecoxib uptake in any of the brain regions or in plasma.

Conclusion: [¹¹C]Rofecoxib can not detect neuroinflammation in our viral encephalitis model and therefore it is not a suitable PET tracer for imaging of COX-2 expression in the brain.

Keywords: Cyclooxygenase-2, Neuroinflammation, Animal PET, [¹¹C]Rofecoxib, Brain

P297 DEVELOPMENT OF NEW TRACERS FOR NONINVASIVE EVALUATION OF IODIDE EFFLUX SYSTEMS IN THE BRAIN**T. OKAMURA, T. KIKUCHI, K. FUKUSHI, K. SUZUKI and T. IRIE**

Department of Molecular Probe, Molecular Imaging Center, National Institute of Radiological Sciences, Chiba, Japan

Introduction: Brain iodide pump (I-pump) actively transports iodide from the brain to the blood, and causes the low concentration of iodide in addition to the limited permeability of the BBB. Intracerebral injection of radioactive iodide is useful for evaluating brain iodide efflux systems (BIES); however, this method is not applicable to human studies. Hence, we devise a novel noninvasive approach for assessment of BIES using SPECT. In this study, five 9-alkyl-6- ^{125}I iodopurines (9R6IPs, R: alkyl) were designed as a proprobe to release iodide by the reaction with GSH. The delivery of radioactive iodide into the brain using 9R6IPs and the manner of iodide efflux from the brain were investigated. Probes should have the following characters: high permeability of the BBB and rapid release of iodide (rapid reaction with GSH).

Experimental: All 9R6IPs were synthesized from the corresponding bromo derivative in a $\text{Br}/^{125}\text{I}$ exchange reaction. The reaction rates of 9R6IPs with GSH in mouse brain homogenate supplemented with 2 mM GSH were examined by TLC/BAS method. The brain kinetics of radioactivity was investigated in ddY mice for 20 min after intravenous injection of 9R6IPs. Brain radioactive metabolites were analysed by TLC and HPLC at 10 min after 9Pe6IP injection. The efflux rate of iodide was estimated by least-square method in the fitting of brain kinetics data to exponential function.

Results and Discussion: The radiochemical yields and purities were 42-56% and more than 96%, respectively. In vitro reaction rates were $0.24\text{--}1.4\text{ min}^{-1}\text{g}^{-1}\text{mL}^{-1}$. When 9R6IPs (R: Bu, Pe, and Bz) with relatively high rates were injected into mice, they registered high uptake at 1 min (2.8-5.3% ID/g tissue) and a decrease from this time-point. 9Pe6IP showed the higher initial uptake as compared to 9Bu6IP and 9Bz6IP. For 9Pe6IP, TLC and HPLC analysis of radioactive metabolites was further performed. TLC analysis confirmed that the radioactivity of the unaltered substance was hardly observed, and HPLC analysis showed that 84% of radioactivity was identical to authentic iodide ($^{125}\text{I}^-$). From these results, the decrease in brain radioactivity would be the clearance of iodide from 10 min post-injection of 9Pe6IP. Effect of I-pump inhibitor perchlorate on the efflux rates was also investigated. The efflux rates decreased in a dose-dependent manner, suggesting that iodide delivered into the brain would be extruded by I-pump from the brain.

Conclusion: Our results demonstrated that 1) 9Pe6IP readily entered the brain, 2) it rapidly released iodide within the brain, 3) after 9Pe6IP disappearance, the clearance of radioactivity represented the efflux of iodide. 9Pe6IP can deliver the radioactive iodide into the brain, leading to noninvasive assessment of BIES.

Keywords: Iodide Pump, Purine, GSH

P298 [^{18}F]-2-FLUOROMETHYL-L-PHENYLALANINE: A NEW TUMOUR TRACER FOR PET. TUMOUR UPTAKE AND BIODISTRIBUTION IN R1M RHABDOMYOSARCOMA BEARING RATS

K. KERSEMANS¹, M. BAUWENS¹, T. LAHOUTTE², C. VANHOVE², A. BOSSUYT² and J. MERTENS¹

¹BEFY/Radiopharm.Chemistry, Vrije Universiteit Brussel, Brussels, Belgium; ²BEFY/ICMIC, Vrije Universiteit Brussel, Brussels, Belgium

Introduction: Many human cancer cells over-express the functional LAT1 transport system that shows high affinity for the uptake of radioiodinated phenylalanine analogues. We developed a new fluorinated phenylalanine analogue, [^{18}F]-2-Fluoromethyl-L-phenylalanine ([^{18}F]-2-Me-L-Phe), that can be prepared with high yield for clinical routine.

Experimental: [^{18}F] - for bromine exchange on the fully protected amino acid analogue (N-Boc, tBut-ester) is performed within 3 minutes in acetonitrile/ $\text{K}_{222}/\text{K}_2\text{CO}_3$ at 120°C with a radiochemical yield of at least 85%. After deprotection (20 minutes at 50°C in $\text{TFA}/\text{CH}_2\text{Cl}_2$: 1/2 and N_2 flow evaporation) [^{18}F]-2-Me-L-Phe was recovered N.C.A with a high radiochemical yield (> 60%) and purity by means of semi-prep RP-HPLC (isotonic saline, pH 7). In vivo imaging of R1M rat rhabdomyosarcoma tumour (volume ranging from 1 cm^3 to 2.7 cm^3) bearing Wag/Rij rats injected with 3.7 MBq of sterile formulation, was performed with a Siemens ACCEL PET camera from 5 to 45 minutes p.i.

Results and Discussion: A high yield and simple radiosynthesis was developed. PET images (Figures 1a. and 1b) show a high uptake in both small and large tumours. As shown in figure 2 the small tumour shows at 15 and 30 minutes the same DUR values as the large tumour. The brain uptake is low as compared to the tumour uptake (tumour/brain ratio of 3.5). Figure 2 confirms the high tumour uptake (tumour/muscle and tumour/heart ratio's of respectively 4.0 and 3.0) and shows that [^{18}F]-2-Me-L-Phe is rapidly cleared from the organs and the rest of the body with a negligible amount of defluorination within the first 30 minutes as demonstrated by absence of skeletal uptake (Figure 1.c. representing the knee-bones). All the imaging results were confirmed by the DAR values of the organs and tissue of interest after dissection.

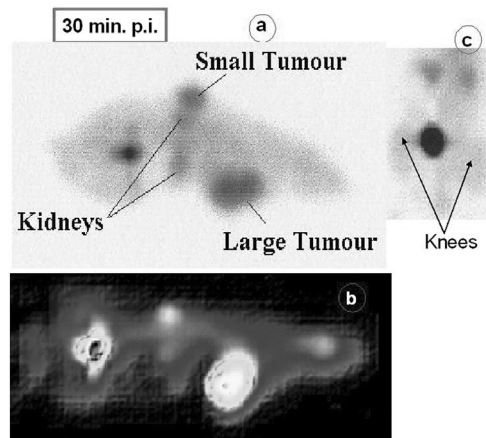


Fig. 1

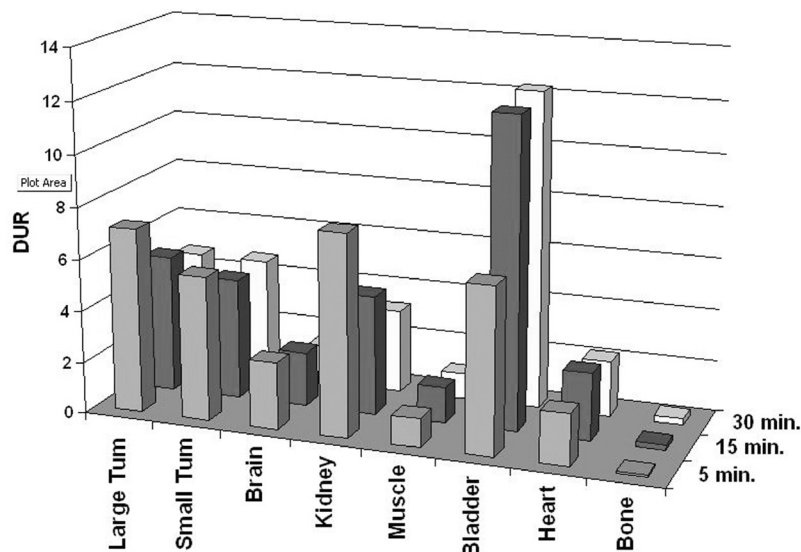


Fig. 2

Conclusion: These results prove that [^{18}F]-2-Fluoromethyl-L-phenylalanine has a great potential as a new tumor specific tracer for PET.

Acknowledgement: The authors thank FWO-Vlaanderen and GOA-VUB for financial support.

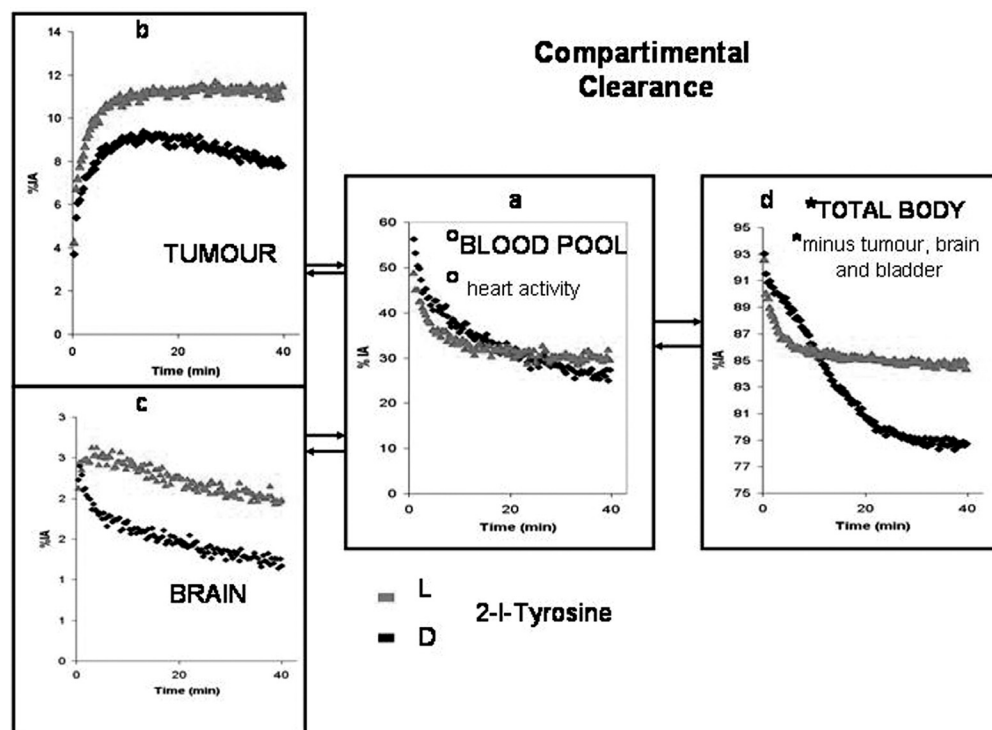
Keywords: Tumour Tracer, [^{18}F]-2-Fluoromethyl-L-Phenylalanine, LAT1 Uptake, PET

P299 COMPREHENSIVE BIODISTRIBUTION OF (123 I)- L AND D-2-I-TYROSINE IN R1M TUMOUR BEARING RATSM. BAUWENS¹, T. LAHOUTTE², K. KERSEMANS¹, A. BOSSUYT² and J. MERTENS¹¹BEFY, Vrije Universiteit Brussel, Brussels, Belgium; ²ICMIC, Vrije Universiteit Brussel, Brussels, Belgium

Introduction: Literature shows that the LAT1 amino acid transporter is overexpressed in many tumour cell lines compared to normal tissue of rats and human, except the blood brain barrier (BBB), large intestins (LI) and kidneys (K). It transports reversibly besides L- also several D- neutral lipophilic amino acid analogues such as 2-I-D-Tyrosine (Tyr). The affinity of 2-I-D-Tyr (Ki: 0.28 mM) for LAT1 expressing R1M rhabdomyosarcoma cells was less than the half of that of 2-I-L-Tyr (Ki: 0.11 mM). Neither the L nor the D-2-I-Tyr analogue was incorporated into proteins. This study describes the pharmacokinetics of [123 I]-L and D-2-I-Tyr in R1M bearing Wag/Rij rats.

Experimental: The presence of LAT1 mRNA (light and heavy chain) was determined by Reverse Transcriptase PCR in several organs/tissues of a Wag/Rij rats and in R1M tumour cells. In vivo the biodistribution in R1M bearing rats (n = 4) of [123 I]-2-Iodo-L-Tyrosine and [123 I]-2-Iodo-D-Tyrosine was performed by dynamic planar imaging with a gamma camera.

Results and Discussion: LAT1 mRNA was present in R1M tumour cells, but not detected in any of the rat tissues. The contribution of LAT1 proteins in BBB, LI and K can be too small for detection. The uptake (% injected activity IA) of D-2-I-Tyr in the tumour (T) and brain (Br) (Fig. 1; b, c) is lower in concordance with the lower affinity. After their maxima the uptake-curves of L and D in T (Fig. 1b) follow the clearance from the blood pool (BP) and the *body (*T, Br and bladder excluded) (Fig. 1, a & d). At longer times, up to 24 hours, T and B cleared for L and D with the same rate of 3.5%/h. Figure 1c shows that the initial activity in Br, linked to cerebral blood flow and BBB passage, is the same for both stereoisomers. The following higher clearance rate of D followed by the fact that up from 20 minutes L and D have about the same efflux rate is related to the clearance of both tracers in the body and BP compartment. The retention of [123 I]-D-2-I-Tyr activity in the *body at longer times (> 1h) is yet not well understood. The related BP clearance depending on reversible kidney filtration and also on deiodination of the iodotyrosine (visible thyroid uptake) does not explain the apparent retention.



Conclusion: RT-PCR revealed LAT1 expression only in the tumours, where the uptake of [123 I]-D-2-I-Tyr is 80% of the L analogue. Its clearance from the body and brain the first hour is faster.

Acknowledgement: FWO-Vlaanderen for financial support.

Keywords: Pharmacokinetics, 2-I-D-Tyrosine, 2-I-L-Tyrosine, LAT1 amino Acid Transport

P300 ^{68}Ga -, ^{86}Y -, AND ^{111}In -RADIOLABELED ANTI-TENASCIN-C OLIGONUCLEOTIDE APTAMERS AS A POTENTIAL PROBE FOR TUMOR IMAGING

M. FRIEBE¹, M. HECHT^{1,2}, S. BORKOWSKI¹, S. SEIFERT², B. NOLL², F. WÜST², A.W. STEPHENS¹, C.S. HILGER¹, R. BERGMANN², B. JOHANNSEN² and L.M. DINKELBORG¹

¹Research Laboratories of Schering AG, Schering AG, Berlin, Germany; ²Institute of Radiopharmacy, Research Center Dresden-Rossendorf, Dresden, Germany

Introduction: The matrix protein tenascin-c (TN-C) represents an interesting target for molecular imaging in oncology due to its high abundance in a variety of human tumors such as lung, breast and brain tumors [1]. First radiolabeled anti-TN-C antibodies could successfully proof the concept of tumor-TN-C targeting [2]. However, a persistently high blood level hampers their use for targeted imaging. Aptamers, a class of rapidly clearing high affinity oligonucleotides, have been introduced successfully to molecular imaging by the application of the Tc-99m labeled TN-C Targeting Aptamer-1 (TTA-1) [3]. Here we report on the radiolabeling, binding affinity and biodistribution of this novel targeting aptamer labeled with metal PET isotopes.

Experimental: Labeling with Ga(III), Y(III), and In(III) was performed in a one pot reaction after conjugation of a DOTA-type chelating moiety to TTA-1-MAG₂. In-111 was included in the study as a surrogate for Ga and Y in long term stability and affinity tests. The labeling was carried out in the presence of the aptamer-chelator conjugate and the respective radiometal in acetate buffer. Degradation was investigated in human plasma employing PAGE. Affinity for human TN-C was determined in a nitrous cellulose filter binding assay. Athymic mice, bearing the human U251 tumor cell line, were injected with the radiolabeled TTA-1 derivatives.

Results and Discussion: Addition of the radiometal salts yielded the respective labeled aptamer conjugates in high yields (60–80%). Ultrafiltration of the products led to > 95% of pure material as determined by PAGE and HPLC methods. The biological stability in human plasma ranged from 68% (In-111) to 95% (Y-86) of intact material after 6 hr. Binding affinity for human TN-C revealed a K_D of 1 nM (In-111). A maximum tumor uptake of 2.0% ID/g (Ga-68), 1 hr p.i. and T/Non Tumor ratios of 5.1 (T/blood), 0.2 (T/kidney), 0.7 (T/liver) 1 hr p.i. proved to be adequate to image the U251 tumor xenograft in mice. Tumor visualization was possible for both Ga-68 and Y-86 labeled TTA-1.

Conclusion: The introduction of a DOTA-type chelating moiety could be successfully used to radiolabel the aptamer probe with In, Ga and Y. The stability against nuclease degradation along with a significant tumor accumulation, high T/blood levels and the imaging capabilities in PET-scans make these compounds promising candidates for further evaluation as multi-tumor imaging agents.

References: 1. R. Chiquet-Ehrismann, *Cell* **47**, 131 (1986). [2] P. Riva, *Cancer* **73**, 1076 (1994). [3] B.J. Hicke, *J. Nuc. Med.* **47**, 668-678 (2006).

Keywords: Aptamers, Oligonucleotides, PET, Ga-68, Tumor Targeting

P301 (^{11}C)-ROMAO – A POTENTIAL NEW PET TRACER FOR THE MAO-A ENZYMER. DI SANTO¹, A.K. OLSEN², K. PEDERSEN², R. COSTI¹, P. CUMMING² and S.B. JENSEN²¹Istituto Pasteur – Fdn "Cenci Bolognietti", Dipartimento Studi Farmaceutici, University of Rome "La Sapienza", Rome, Italy; ²PET-Centre, Aarhus University Hospital, Aarhus C, Denmark

Introduction: Monoamine oxidase (MAO) is responsible for the metabolism of dopamine, serotonin and other primary amines, and is the target for an important class of antidepressants. In recent years, a few reversibly-binding radioligands for the detection of MAO types A and B by positron emission tomography (PET) have become available. However, these ligands are not optimal due to difficult synthesis or due to rapid metabolism in blood. We have screened a number of pyrrolylethanamines and pyrrolylethanolamines *in vitro*[1] as potential candidates for MAO-A and -B tracers. The most promising compound identified (ROMAO) was chiral; we synthesized both precursors and both reference compounds in order to test their suitability as PET ligands. The R-form had 200.000-fold selectivity for MAO-A over MAO-B, whereas the S-form had 50.000-fold selectivity.

Experimental: For the PET-study, carbon-11 methylation of the pyrrol ring of the precursors were undertaken with *N,N*-dimethylformamide (DMF) as the solvent and sodium hydride (NaH) as the base. The products (-)-(R)- and (+)-(S)-1-(1-methyl-1*H*-pyrrol-2-yl)-2-phenyl-2-(pyrrolidin-1-yl)ethanone (R- and S-ROMAO) were purified by semi-preparative HPLC, before quality control. The radiochemical purity of [^{11}C]S- and [^{11}C]R-ROMAO was higher than 98%, and the radiochemical yield was 20-40%, relative to the collected [^{11}C]methyl iodide. The specific radioactivity of both [^{11}C]ROMAO enantiomers was around 80 GBq/ μmol .



Results and Discussion: Danish Landrace/Yorkshire pigs (38 - 41 kg) were anaesthetized and placed in the ECAT EXACT tomograph. Emission recordings were obtained during 90 min. after injection of 200-400 MBq tracer. Results of the scans showed that both R- and S-ROMAO entered into brain, but were also eliminated very rapidly from circulation. HPLC fractionation of plasma extracts showed that ca. 20% of the total radioactivity was untransformed tracer at 30 min. post injection.

Conclusion: Preliminary image analysis showed a pattern of uptake in brain which was not identical to, but resembling the distribution in pig brain of the MAO-A ligand [^{11}C]harmine[2]. The cerebral distributions of R- and S-ROMAO were similar, and characterized by incomplete blocking in a pilot study with pargyline treatment. We are currently investigating the kinetics of the cerebral binding of the two [^{11}C]-ROMAO enantiomers.

Keywords: Monoamine Oxidase (MAO), PET Study, ROMAO

P302 INTERNALIZATION, EFFLUX, AND DOSIMETRY OF TWO ^{64}Cu -LABELED SOMATOSTATIN ANALOGS IN A HUMAN SSTR2-TRANSFECTED CELL LINE

M. EIBLMAIER¹, R. LAFOREST¹, J.J. PARRY², R. ANDREWS², B.E. ROGERS² and C.J. ANDERSON¹

¹Mallinckrodt Institute of Radiology, Washington Univ. School of Medicine, St. Louis, MO, USA; ²Department of Radiation Oncology, Washington Univ. School of Medicine, St. Louis, MO, USA

Introduction: Over the last decade, the somatostatin receptor (SSTR) has become established as a target of cancer pharmaceuticals. Clinical trials were performed with ^{90}Y -DOTATOC and ^{177}Lu -DOTATATE in patients with neuroendocrine tumors and have shown promising results. ^{64}Cu has decay characteristics (β^+ : 19%, β^- : 40%, $T_{1/2}$ = 12.7 h) suitable for both PET imaging and targeted radiotherapy. We acquired internalization and efflux profiles of two somatostatin analogs, ^{64}Cu -TETA-Y3-TATE (**1**) and ^{64}Cu -CB-TE2A-Y3-TATE (**2**) in A427 human non-small cell lung carcinoma cells stably transfected with SSTR2 (A427-7). The two chelators TETA and CB-TE2A are known to have different *in vivo* stabilities. Absorbed doses from **1** and **2** to A427-7 cells were compared with results from external beam radiation.

Experimental: Internalization of **1** or **2** into A427-7 cells during a pulse of 4h and efflux during the following 20h were monitored. At various time points, ^{64}Cu activities in the medium, the cell lysate and on the cell surface were measured. Internalization/efflux data in dps/cell and previous nuclear uptake experiments were used to calculate absorbed dose to cells and nuclei. A427-7 cells were irradiated using a PANTAK pmc1000 X-ray machine, and the effects of external beam radiation determined via a colony formation assay.

Results and Discussion: Surface binding and internalization were substantially higher for **2** compared to **1**, which is in accord with previous findings. Internalized activity peaked at 3h, and there was no efflux observed for either compound over the next 20h. The absorbed dose to A427 cells was 0.40 Gy for **1**, and 1.06 Gy for **2**. The nuclear uptake for **1** was higher than **2** at 12 and 24h; however, this did not significantly contribute to the overall dose to cells. These surprisingly low numbers are due to the size of A427-7 cells (19 μm) rather than inadequate uptake of drug. Data from external beam radiation suggests that absorbed dose from either radiopharmaceutical is too low for efficient cell killing (<10% cell killing at 1 Gy).

Conclusion: Due to their size, A-427 cells may not be ideal for investigating cell killing by ^{64}Cu -labeled somatostatin analogs. Nevertheless, lack of ^{64}Cu efflux from these cells suggests that both **1** and **2** can permanently import the radiometal into human cells, so that imaging applications, and therapy in other model systems, merit evaluation.

Acknowledgement: The authors thank S. Adams for technical assistance and S.M. Goddu for helpful discussion on dosimetry. Funding was provided by National Institutes of Health grants 5 R01 CA064475 (CJA), R01 EB004533 (BER) and R24 CA86307 (^{64}Cu production).

Keywords: Copper-64, PET Imaging, Targeted Radiotherapy, Somatostatin Receptor, Somatostatin Analog

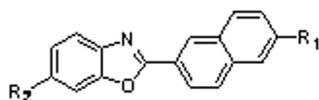
P303 NEW ^{18}F -LABELED TARGETING AGENTS FOR ABETA AGGREGATES BASED ON THE FLUORESCENT BENZOXAZOLE-NAPHTHYL CORE

K.A. STEPHENSON, C. HOU, M. KUNG and H.F. KUNG

University of Pennsylvania, Philadelphia, PA, USA

Introduction: Alzheimer's disease (AD) is a neurodegenerative disease of the brain characterized by dementia, cognitive impairment and memory loss. Currently there is no simple, definitive imaging tool available to assist the diagnosis of AD. Imaging Abeta plaques in vivo will improve AD diagnosis by identifying patients with excess Abeta plaques in the brain and therefore likely to develop AD. In addition to diagnosis imaging the progression of the disease may prove to be essential in monitoring treatment. During the last 5 years there have been several Abeta specific biomarkers proposed for PET imaging including [^{11}C]-PIB and [^{11}C]-SB-13(1,2). Unfortunately carbon-11 labeled probes are limited because of the radioisotope's short half-life, therefore the development of ^{18}F ligands for Abeta are of interest.

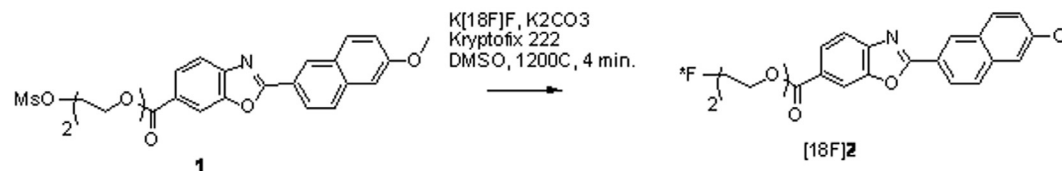
Experimental: A series of new compounds based on the benzoxazole-naphthyl core (Figure 1) were prepared, Ki values measured, and their fluorescent properties in ethanol and water determined. [^{18}F]**2** was then prepared via nucleophilic displacement of the mesylate precursor with [^{18}F]fluoride in 35% decay corrected radiochemical yield and 98% purity with specific activity (E.O.S. = 700 Ci/mmol). The biodistribution of [^{18}F]**2** was then evaluated in normal mice.



$\text{R}_1 = \text{OMe}, \text{OH}, \text{NH}_2, \text{NHMe}, \text{NMe}_2$

$\text{R}_2 = \text{Me}, \text{COOH}, \text{COOMe}, \text{COO}(\text{PEG})_n\text{OH}, \text{COO}(\text{PEG})_n\text{F} \ (n=2-4)$

Fig. 1



Scheme 1. Radiosynthesis of [^{18}F]**2**

Results and Discussion: In order to help improve the solubility of the benzoxazole-naphthyl core and provide a convenient place to incorporate ^{18}F , a series of short polyethyleneglycol (PEG) chains were incorporated without affecting the highly desirable nanomolar binding affinities for Abeta aggregates (Ki values ranged between 5–40 nM, determined in an assay using postmortem AD brain homogenates). Compound **2** was selected for radiolabeling based on its nanomolar binding affinity, low molecular weight and favorable fluorescent properties. Utilizing the fluorescence of these compounds we then labeled Abeta aggregates in transgenic mouse brain sections and co-registered the autoradiographic and fluorescent microscopy images of [^{18}F]**2** and **1**. The in vivo biodistribution of [^{18}F]**2** was also performed in normal mice, and demonstrated good brain uptake (3.87% ID/g at 2 min postinjection).

Conclusion: Based on our preliminary results with [^{18}F]**2**, we believe these novel pegylated benzoxazole-naphthyl compounds show promise as new core structures targeting Abeta aggregates.

References: [1] Klunk, W.E.; et. al. *Ann Neurol.*, 2004, 55: 306. [2] Verhoeff, N.P.; et. al. *Am. J. Geriatr. Psychiatry.* 2004, 12: 584.

Keywords: PET Imaging, Alzheimer's Disease, Fluorine-18

P304 SYNTHESIS AND EVALUATION OF (¹¹C)LANIQUIDAR, A POTENTIAL NEW PET LIGAND FOR MEASURING P-GLYCOPROTEIN IN THE BLOOD-BRAIN BARRIER

G. LUURTSEMA, R.C. SCHUIT, R.P. KLOK, J.D.M. HERSCHEID, S.C. BERNDSEN, J. VERBEEK, J.E. LEYSEN, A.A. LAMMERTSMA and A.D. WINDHORST

Department of Nuclear Medicine & PET Research, VU University Medical Centre, Amsterdam, Netherlands

Introduction: Recently, (*R*)-[¹¹C]verapamil has been developed as a ligand for functional P-glycoprotein (P-gp) in the blood-brain barrier (BBB). Verapamil is a substrate for P-gp, resulting in low uptake in normal brain. In case of overexpression of P-gp, which might be associated with drug resistance, uptake will be even lower, resulting in poor counting statistics. To measure overexpression, a better strategy would be to use a specific antagonist of P-gp, such as laniquidar. Laniquidar is not a substrate and overexpression should lead to increased uptake.

The purpose of the present study was to label laniquidar with carbon-11 and to evaluate [¹¹C]laniquidar as a tracer of P-gp in normal rats.

Experimental: The synthesis of [¹¹C]laniquidar was performed by addition of [¹¹C]CH₃I to 2.0 mg of carboxylic precursor dissolved in 300 µL of DMSO containing 1.2 µL of 60% TBAH. The product was purified by HPLC (Waters µBondapak 7.8x300 mm; water/acetonitrile/TFA 68/32/0.1, 4.5 ml/min). Reformulation over a tC₁₈ Seppak yielded a sterile solution of [¹¹C]laniquidar in saline. Rats received a injection of 20 MBq [¹¹C]laniquidar in the tail vein, and were sacrificed at 5, 15, 30 and 60 minutes. Several tissues and distinct brain regions were dissected and counted for radioactivity. In addition, the biodistribution of [¹¹C]laniquidar in rats pre-treated with cyclosporine A was measured 30 minutes p.i. Finally, the metabolic profile of the tracer in plasma was determined.

Results and Discussion: The optimal reaction time was 2 minutes at 60°C, providing a yield of 30% (c.f.d.) and a (radio)chemical purity of >99%. SA was 40-60 GBq/µMol at time of injection.

At 30 minutes, the % i.d./g of tracer in lung, liver, spleen, kidney and whole brain was 4.49±1.92, 2.10±0.22, 1.76±0.16, 1.08±0.04 and 0.06±0.01, respectively. In the pre-treated rats the brain uptake was significantly higher. The ratios (cyclosporine A/normal) in cerebellum, hippocampus, cortex and striatum were 7.87, 5.80, 8.94 and 7.89, respectively. Metabolite analysis showed that 70% of activity in plasma was still parent compound, 30 minutes after tracer injection.

Conclusion: [¹¹C]laniquidar can be synthesized in sufficient amounts for *in vivo* PET studies. Uptake in the brain was, however, low and significantly increased after administration of cyclosporine A. The *in vivo* rate of metabolism was relatively low. Further studies are needed to investigate the antagonistic behaviour of [¹¹C]laniquidar and to assess whether uptake is specific for P-gp.

Acknowledgement: The EC - FP6-project DiMI, LSHB-CT-2005-512146 is acknowledged for financial contribution and J&J for providing Laniquidar.

Keywords: Synthesis, Evaluation, P-gp Ligand, Rats, PET

P305 ^{76}Br - OR ^{64}Cu -LABELED ANTIBODY FOR IMMUNO-PET IN QUANTITATIVE EVALUATION OF RADIOIMMUNOTHERAPY

Y. IIDA¹, H. HANAOKA¹, N.S. ISHIOKA², T. KATABUCHI^{2,3}, S. WATANABE², S. WATANABE^{2,3}, S. MATSUHASHI², T. HIGUCHI⁴, N. ORIUCHI⁴ and K. ENDO⁴

¹Bioimaging Information Analysis, Gunma University Graduate School of Medicine, Maebashi, Gunma, Japan; ²Radiation-Applied Biology, Japan Atomic Energy Agency, Takasaki, Gunma, Japan; ³21st Century COE Program, Gunma University Graduate School of Medicine, Maebashi, Gunma, Japan; ⁴Diagnostic Radiology and Nuclear Medicine, Gunma University Graduate School of Medicine, Maebashi, Gunma, Japan

Introduction: Radioimmunotherapy (RIT) is one of the most promising treatments for cancer therapy. Recently, though RIT becomes available for clinical use and shows high efficacy, it has some adverse effects for radiation to normal tissues, and its therapeutic window is limited. So, assessment of radiation dose to both tumor and normal tissues is very important for RIT. PET is superior in quantitative measurement and it can estimate radiation dose directly. Although several positron emitters have been used for PET, they don't suit for labeling of antibody because of their short half-lives. Compared with these radionuclides, ^{76}Br and ^{64}Cu have appropriate properties (^{76}Br : $T_{1/2} = 16.1\text{hr}$, ^{64}Cu : $T_{1/2} = 12.7\text{hr}$) and they may have great potentials for immuno-PET. ^{76}Br or ^{64}Cu labeled antibody is also suitable for evaluation of cancer therapy. In this study, we synthesized anti-CD20 monoclonal antibody (mAb), NuB2, labeled with ^{76}Br or ^{64}Cu , and evaluated potential for in vivo quantitative evaluation of RIT.

Experimental: Direct bromination similar with iodination of proteins has been applied for ^{76}Br labeling of NuB2. For labeling with ^{64}Cu , a stable immunoconjugate was prepared by reacting NuB2 with 1,4,8,11-tetraazacyclotetradecan-N,N',N'',N'''-tetraacetic acid (TETA). For in vivo biodistribution and tumor localization studies, ^{76}Br or ^{64}Cu labeled NuB2 was prepared and administered to SCID mice bearing CD20+ tumor. We also performed imaging study with PET at 24hr after injection of radiolabeled NuB2.

Results and Discussion: Radiochemical yield of ^{76}Br -NuB2 was approximately 10% and that of ^{64}Cu -TETA-NuB2 was approximately 90%. The results of tumor localization studies show that the tumor concentration of radioactivity increased steadily throughout the course of experiment for both compounds, and reached to 5%dose/g for ^{76}Br -NuB2 and 17%dose/g for ^{64}Cu -TETA-NuB2 at 2 days. Same results were also obtained from PET studies.

Conclusion: In this study, we successfully prepared radiolabeled mAbs for PET, exhibiting high affinity for CD20+ tumor. ^{76}Br -NuB2 and ^{64}Cu -TETA-NuB2 were highly accumulated to tumor, and PET could show these images clearly, which were same results with ex vivo studies. Lower tumor uptake of ^{76}Br -NuB2 seems to be owing to dehalogenation. From these data, the use of ^{76}Br and ^{64}Cu for immuno-PET has potential for accurately evaluation of RIT.

Keywords: Antibody, PET, Br-76, Cu-64, Radioimmunotherapy

P306 TOWARDS THE FLUORINE-18 LABELLING OF NEW MMP RADIOLIGANDS: LABELLING OF 2-FLUOROPYRIDINE-BASED PHOSPHINIC BUILDING BLOCKS

B. KUHNAST¹, F. DOLLE¹, F. HINNEN¹, B. TAVITIAN¹, V. DIVE² and L. DEVEL²

¹Service Hospitalier Frédéric Joliot, CEA/DSV, Orsay, France; ²Département d'Ingénierie et d'Études des Protéines, CEA/DSV, Gif sur Yvette, France

Introduction: Matrix metalloproteinases (MMPs) are a family of zinc dependent enzymes that play an important role in cancer progression as well as in numerous diseases. Non-invasive imaging of MMPs with PET would allow the detection of MMP active forms in cancer and the assessment of the response in MMP inhibitor based therapies. A new series of phosphinic peptides, bearing both an aromatic moiety at the P1-position and a substituted isoxazole at the P'1-position has been described as highly potent specific MMP-12 inhibitors [1]. To image this class of inhibitors, new building blocks bearing a pyridine, prone to labelling with fluorine-18, have been synthesized. We report here preliminary results on the labelling of one of these new building blocks.

Experimental: 500 µL of DMSO containing 8.8-11.1 µmol of **2** were added to the dried K[¹⁸F]F-K₂₂₂ complex. The reaction mixture was heated 15 min at 170°C. A 5%-aliquot (about 450 MBq, decay corrected) of this mixture was diluted with 5 mL of aq. HCl (0.5N) and passed through an EtOH-activated C-18 Seppak cartridge. Elution of the cartridge was performed using EtOH containing 0.2% aq. ammonia (2 mL). This eluate was finally analyzed by analytical RP-HPLC.



Results and Discussion: Using the non-optimized conditions described above, about 50% of the radioactivity is fixed on the cartridge from which elution with the ammonia/EtOH solution allowed to recover 50% of the fixed activity. HPLC analysis of the latter eluate shows three radioactive peaks eluting at 2.7 min, 9.3 min and 13.6 min and representing 30%, 60% and 10% of the injected radioactivity, respectively. Co-injection with reference compound **1** was performed, allowing to demonstrate that the peak eluting at 9.3 min is [¹⁸F]-**1**. Based on these results, decay corrected yields for the preparation of [¹⁸F]-**1** is 15%. Further experiments are currently underway to optimize these conditions and to fully robotize (Zymate XP) the process on a whole radioactive reaction batch.

Conclusion: These preliminary results confirm the easy access to fluorinated pyridine-based phosphinic building blocks bearing a substituted isoxazole moiety. The next step includes the carboxylic acid functionalization in order to label MMP-12 inhibitors.

Reference: [1] Devel L. et al, J Biol Chem (2006), 28: 1152.

Acknowledgement: This project was in part supported by FP6RDT (Cancer Degradome project, LSHC-CT-2003-50297).

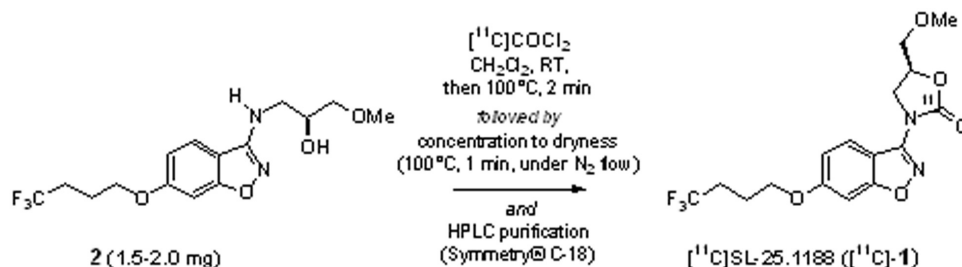
Keywords: Fluoropyridine, MMP Inhibitors, Phosphinic Peptides

P307 RADIOSYNTHESIS OF (S)-5-METHOXYMETHYL-3-(6-(4,4,4-TRIFLUOROBUTOXY)-BENZO(d)ISOXAZOL-3-YL)-OXAZOLIDIN-2-(¹¹C)ONE (¹¹C)SL-25.1188), A NOVEL RADIOLIGAND FOR IMAGING MONOAMINE OXIDASE-B WITH PET

Y. BRAMOULLE¹, F. PUECH², W. SABA¹, H. VALETTE¹, M. BOTTLAENDER¹, P. GEORGE² and F. DOLLE¹

¹Service Hospitalier Frédéric Joliot, CEA/DSV, Orsay, France; ²Sanofi-Aventis, Bagneux, France

Introduction: In the last decade, a novel series of 2-oxazolidinones has been developed by Sanofi-Aventis as highly potent monoamine oxidase (MAO) inhibitors. Within this series, befloxatone, initially selected on its pharmacological profile (K_i (rat/human): 1.9-3.6 nM for MAO-A and ED_{50} (rat): 0.1-0.2 mg/kg p.o.), has been successfully labelled using [¹¹C]phosgene and characterized in non-human primates (1,2) as a potent radioligand for imaging MAO-A with PET. SL-25.1188, another 2-oxazolidinone derivative, inhibits selectively and competitively MAO-B in human- and rat brain (K_i values of 2.9 and 8.5 nM, respectively and ED_{50} (rat): 0.6 mg/kg p.o.) (3). Considered an appropriate candidate for imaging MAO-B with PET, SL-25.1188 was labelled with [¹¹C]COCl₂ at its oxazolidinone function.



Experimental: The conditions used were the following: (a) trapping at RT of [¹¹C]COCl₂ in CH₂Cl₂ (0.5 mL) containing **2** (1.5-2.0 mg); (b) heating at 100°C for 2 min; (c) concentration to dryness at 100°C under a N₂ stream and taking up the residue in 0.5 mL of MeCN; (d) dilution with 0.5 mL of water containing HNEt₂ (4% v:v) and (e) purification using semi-preparative HPLC (Symmetry C-18).

Results and Discussion: Compared to [¹¹C]befloxatone, surprisingly low RCYs (1.1-4.0%, decay-corrected, n = 20) were observed whatever the conditions used. Different amounts of precursor (1.0-7.0 mg), solvents (MeCN, toluene, CH₂Cl₂), temperatures and reaction times (RT to 130°C, 0.5-5.0 min) were tried, the optimal conditions being those described above in the experimental section.

Conclusion: Typically, starting from a 0.7 Ci (25.9 GBq) [¹¹C]CH₄ production batch, about 10 mCi (370 MBq) of [¹¹C]-**1** were obtained within 30 min (Sep-pak-based formulation incl.) with specific radioactivities ranging from 1.2 to 1.7 Ci/micromol (44.4-62.9 GBq/micromol). No attempts have been made to date to further optimize these reactions, as sufficient material was obtained to allow for preliminary radiopharmacological characterization.

References: [1] Dolle F. et al., *Bioorg. Med. Chem. Letters* 2003, 13 (10), 1771-1775. [2] Bottlaender M. et al., *J. Pharmacol. Exp. Ther.* 2003, 305 (2), 467-473. [3] Curet O. et al., 29th Ann. Meet. Soc. Neurosci. - USA (Los Angeles, USA, 23-28/11/1999, # 848.14).

Keywords: SL-25.1188, Carbon-11, Phosgene, MAO-B

P308 SYNTHESIS OF I-124 LABELED 2-(¹²⁴I)IODOHYPERICIN AND MICRO PET IMAGE OF 9L GLIOMA BEARING NUDE MICE

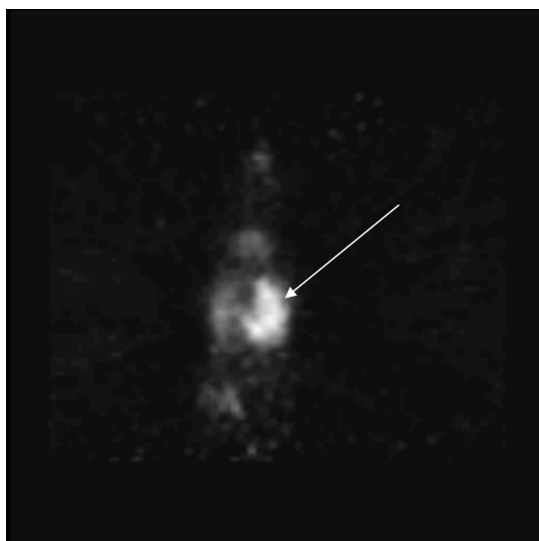
S.W. KIM¹, J.H. PARK¹, M.G. HUR¹, S.D. YANG¹, G.S. WOO², C.W. CHOI² and K.H. YU³

¹Radiation Application Division, Korea Atomic Energy Research Institute, Jeongup, Jeollabuk-do, Republic of Korea; ²Nuclear Medicine, Korea Institute of Radiological and Medical Sciences, Seoul, Republic of Korea; ³Chemistry, Dongguk University, Seoul, Republic of Korea

Introduction: Hypericin which has been isolated mainly from plant of the *Hypericum Perforatum* (St. John's wort) is aromatic polycyclic dione. St. John's wort has been used for the treatment of depression and wound-healing agent. It has been shown to have important antiretroviral activity against several types of viruses and photo-toxicity against some tumor cells including glioma. We showed that 2-[¹²³I]iodohypericin has a possibility to be used as a brain tumor imaging agent from *in vitro* results with C-6, U-251 and U-373 glioma cell line. The present study is to investigate the possibility of 2-[¹²⁴I]iodohypericin as a glioma imaging agent.

Experimental: The reference compound, 2-iodohypericin, has been prepared by the reaction of hypericin with sodium iodide. I-124 was produced using the [¹²⁴Te]TeO₂ target. 2-[¹²⁴I]iodohypericin was prepared similar to previously reported methods for 2-[¹²³I]iodohypericin. 2-[¹²⁴I]iodohypericin was separated and collected on an X-terra RP 18 column. 9L glioma cell line was grafted to nude mice. The nude mice was anesthetized by ether and 2.96 MBq of 2-[¹²⁴I]iodohypericin was injected into a tail vein. The micro PET image was acquired with Concorde animal PET for 30 min at 30 min post injection.

Results and Discussion: The labeling yield was about 60 ± 5% and the optimal reaction time was 10 min at room temperature. The radiochemical purity of 2-[¹²⁴I]iodohypericin was about 97% after purification. Significant uptake of 2-[¹²⁴I]iodohypericin was seen in the tumor transplanted mice.



Conclusion: This is the first study to show the possibility to use a 2-[¹²⁴I]iodohypericin as a brain tumor imaging agent using micro PET and further study is ongoing.

Acknowledgement: This research was performed for the Nuclear R&D Programs funded by the Ministry of Science & Technology(MOST) of Korea.

Keywords: Hypericin, I-124, PKC, Glioma, PET

P309 IMPROVED AND GMP-COMPLIANT RADIOSYNTHESIS OF (^{11}C)DOCETAXEL AND ITS PURIFICATION

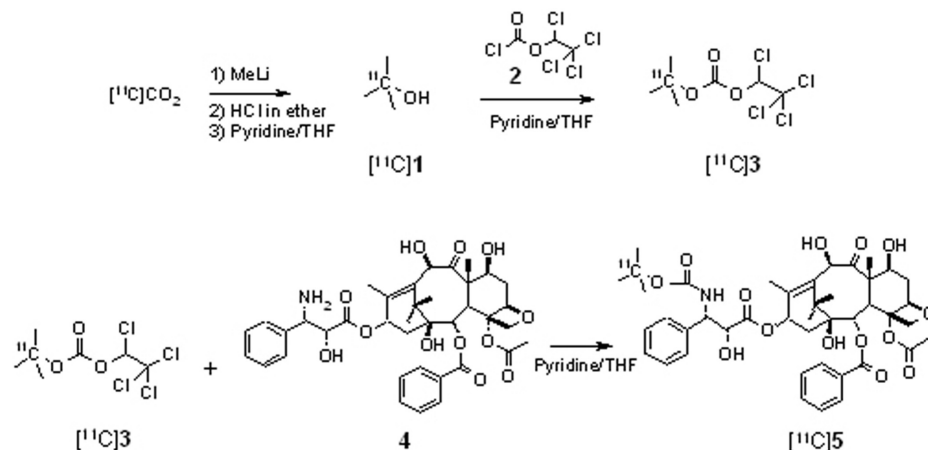
M.P.J. MOOIJER, E.W. VAN TILBURG, N.H. HENDRIKSE, A.A. LAMMERTSMA and A.D. WINDHORST

Nuclear Medicine & PET Research, VU University Medical Center, Amsterdam, Netherlands

Introduction: Docetaxel (Taxotere) is an chemotherapeutic agent for the treatment of breast cancer and non-small cell lung cancer. However, only around 50% of patients respond to treatment. Clearly, there is a need for a method that can predict response to docetaxel treatment. In theory, assessment of tumour uptake of [^{11}C]docetaxel using PET could be such a response predictor. The radiosynthesis of [^{11}C]docetaxel has been described previously¹, albeit without its purification and formulation.

The aim of the present study was to improve the radiosynthesis of [^{11}C]docetaxel ([^{11}C]5, Scheme 1), develop its purification and formulation, and to set up a GMP compliant production.

Experimental: First, the formation of [^{11}C]1 was improved by a reduced amount of MeLi compared to the quenching agent HCl. Neutralization was achieved by adding a pyridine/THF mixture to improve distillation of [^{11}C]1. For the formation of [^{11}C]3 THF was used instead of DCM. Next, removal of the excess of 2 was optimised by replacing the Sep-Pak tC18 with two Sep-Pak amino propyl (NH_2) cartridges. For that purpose, 50 μl of H_2O was added to the crude reaction mixture in order to dissolve all salts that could be present. Thereafter, the mixture was purged with 0,8 ml of THF through the Sep-Pak cartridges, eluting [^{11}C]3 and leaving 2 behind. In this way the unwanted hydrolysis of [^{11}C]3 was reduced. The eluted [^{11}C]3 was collected in a third reaction vial that contained 4 (75 mg) in pyridine (200 μL) and the mixture was heated at 65°C for 7 min, yielding [^{11}C]5. The product was purified by semi preparative HPLC (XTerra 250x50 mm, Acetonitrile/0,1M Ammonium phosphate 50/50, 50 ml/min). The fraction containing the product was diluted with 150 ml of water and passed over a tC18 seppak. After washing the Seppak with 20 ml of water, the product was eluted with 1 ml of ethanol and 14 ml of 7.09 mM of NaH_2PO_4 in saline (pH 5) to yield a sterile solution of [^{11}C]5.

Scheme 1. Radiosynthesis of [^{11}C]Docetaxel.

Results and Discussion: [^{11}C]Docetaxel was obtained in an overall decay corrected radiochemical yield of $10 \pm 2\%$ ($n=12$) with a specific activity of 9-17GBq/ μmol at the end of synthesis (67min after EOB).

Conclusion: The synthesis of [^{11}C]docetaxel was improved to a more reproducible and GMP-compliant method, which is now available for human application.

Acknowledgement: The BV Cyclotron VU is acknowledged for providing $^{11}\text{CO}_2$

References: [1] E.W. van Tilburg *et al.*, J Label Compd Radiopharm 2004; **47**: 763-777.

Keywords: [C-11]Docetaxel, [C-11]-T-Butanol, GMP Compliant

P310 RADIOIODINATED PYRIMIDINE-2,4,6-TRIONES AS MODEL PROBES FOR THE *IN VIVO* MOLECULAR IMAGING OF ACTIVATED MMPs

K. KOPKA¹, H.-J. BREYHOLZ¹, S. WAGNER¹, W. BRANDAU², S. HERMANN¹, O. SCHOBER¹, B. LEVKAU³, C. BREMER⁴ and M. SCHAEFERS¹

¹Department of Nuclear Medicine, University Hospital Muenster, Muenster, Germany; ²Department of Nuclear Medicine, University Hospital Essen, Essen, Germany; ³Institute of Pathophysiology, Center of Internal Medicine, University Hospital Essen, Essen, Germany; ⁴Department of Clinical Radiology, University Hospital Muenster, Muenster, Germany

Introduction: Matrix metalloproteinases (MMPs) are zinc-dependent endopeptidases and involved in the proteolytic degradation of the extracellular matrix. MMPs participate in many diseases, such as inflammation, cancer and atherosclerosis. Radioligands based on nonpeptidyl MMP inhibitors (MMPIs), such as HO-[¹²³I]-CGS 27023A, have been suggested as potential tracers for the *in vivo* molecular imaging of activated pathophysiologically relevant MMPs. We here present the pyrimidine-2,4,6-triones as potential alternative class of nonpeptidyl MMPI radioligands.

Experimental: We identified the barbiturate 5-[4-(2-Carboxyethyl)piperazin-1-yl]-5-[4-(4-iodophenoxy)phenyl]-pyrimidine-2,4,6-trione (I-Barb-COOH, clog D = 1.07) that possesses a high MMP binding potency for activated gelatinases A and B, MMP-2 and -9 (IC₅₀=1-29 nM). Radiosyntheses of the ¹²³I- and ¹²⁴I-labelled versions of I-Barb-COOH were realised (Figure 1) and provided for preliminary evaluation in MMP-rich tumour bearing mice using *in vivo* scintigraphy and small-animal PET (quadHIDAC).

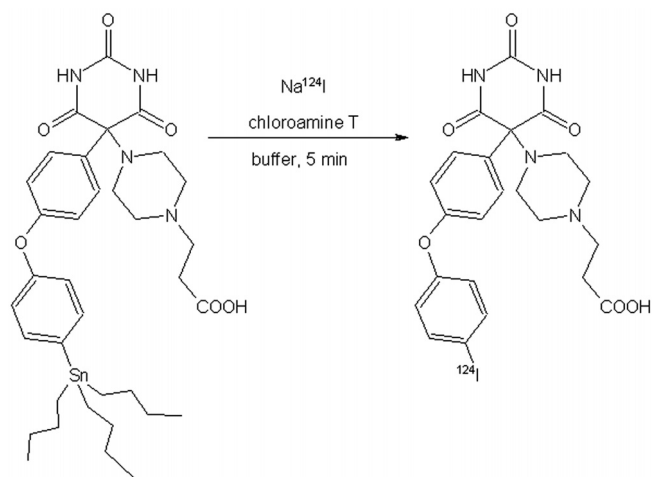


Fig. 1

Results and Discussion: Using the highly sophisticated radioiodinated versions of I-Barb-COOH, we were able to *in vivo* image MMP-rich HT-1080 fibrosarcomas, xenografted into athymic nude mice, by small-animal PET. The PET-compatible ¹²⁴I-labelled model tracer begins to accumulate into the tumours 24 h after injection, giving the best tumour-to-background ratio not until 6 d. Exemplarily, we have shown the potency of tracer accumulation by blocking experiments using [¹²³I]-Barb-COOH in M21 melanoma bearing mice and gamma counting of the explanted tumours.

Conclusion: The here presented class of barbiturate-based MMPI radiotracers evolves into molecular imaging probes for the noninvasive visualisation of activated MMPs *in vivo*. The preliminary *in vivo* experiments encourage to further modify this class of MMP imaging agent aiming at the improvement of the pharmacokinetics to obtain corresponding scintigraphic images within hours, not days.

Acknowledgement: The work is supported by the Deutsche Forschungsgemeinschaft (DFG), Sonderforschungsbereich 656 MoBil, Muenster, Germany (project A2).

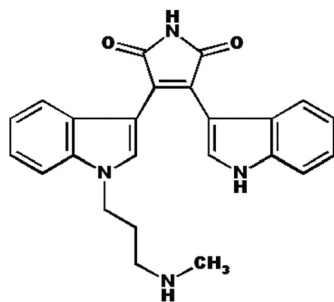
Keywords: Molecular Imaging, Matrix Metalloproteinases, Barbiturates, MMP Inhibitors, *In Vivo* Scintigraphy

P311 SYNTHESIS AND BIODISTRIBUTION OF (¹¹C)METHYL-BISINDOLYLMAREIMIDE III, A INHIBITOR OF PROTEIN KINASE C

K. TAKAHASHI¹, K. KUDO², M. OKADA¹, K. YANAMOTO¹, A. HATORI¹, T. IRIE¹, K. SUZUKI¹ and S. MIURA²

¹Molecular Imaging Center, National Institute of Radiological Sciences, Chiba, Japan; ²Radiology and Nuclea Medicine, Akita Research Institute of Brain and Blood Vessels, Akita, Japan

Introduction: Protein kinase C (PKC) was thought to be involved in a conserved ischemic response pathway (Bright R., et al. 2006. Stroke. 36, 2781). We attempted to label [¹¹C]methyl-Bisindolylmareimide III (BIM1) which was expected to be a inhibitor of PKC (Toullec D., et al. 1991. J Biol Chem. 266, 15771) with expectation that [¹¹C]BIM1 could measure PKC in ischemic brain tissues by PET.



Structure of BIM1.

Experimental: N-methylation of bisindolylmareimide III hydrochloride with [¹¹C]iodomethane was carried out in DMF at 80°C for 90 sec with trace amount of NaOH. The product was purified using a preparative reversed phase HPLC. After evaporation of solvent, the residue was dissolve saline. Tissue distribution of [¹¹C]BIM1 was carried out with dissection method in mice.

Results and Discussion: The radiochemical yield was 30-50% based on [¹¹C]CO₂ and the radiochemical purity was better than 95% measured by HPLC and TLC. The over all time of synthesis was 30 min after EOB. Liver and kidney show high uptakes, which should mean fast metabolism and fast excretion of this tracer. Brain uptake was much lower than that in blood.

Tissue uptakes of radioactivity (% dose/g tissue) mice, n=3

tissues	2 min	15 min	30 min	60 min
Blood	2.50 ± 0.25	0.78 ± 0.20	0.67 ± 0.10	0.73 ± 0.52
Heart	3.57 ± 0.32	3.08 ± 0.60	2.68 ± 0.20	1.37 ± 0.33
Lung	10.75 ± 1.65	4.26 ± 1.01	3.97 ± 0.49	2.46 ± 0.70
Liver	30.13 ± 1.44	23.21 ± 4.22	16.91 ± 1.93	8.76 ± 1.96
Spleen	4.85 ± 0.62	2.69 ± 0.64	2.16 ± 0.30	1.21 ± 0.21
Kidney	40.01 ± 1.67	37.32 ± 5.43	35.17 ± 1.42	22.85 ± 3.44
S.Intenstine	4.49 ± 1.50	9.59 ± 3.46	5.90 ± 1.24	5.86 ± 2.07
Testis	0.13 ± 0.01	0.21 ± 0.03	0.25 ± 0.03	0.24 ± 0.04
Muscle	0.87 ± 0.12	1.05 ± 0.21	1.15 ± 0.14	0.73 ± 0.18
Brain	0.17 ± 0.01	0.20 ± 0.02	0.23 ± 0.04	0.20 ± 0.04

Conclusion: These results suggest that [¹¹C]BIM1 would not be suitable for measuring PKC in the living human brain with PET.

Keywords: Bisindolylmareimide, PKC, Carbon 11, Intracellular Signal Transduction

P312 SYNTHESIS AND CHARACTERIZATION OF ^{86}Y -, ^{68}Ga - AND ^{111}In -CHXA"- ReCCMSH(Arg¹¹) MELANOMA TARGETING PEPTIDES

L. WEI¹, X. ZHANG², C. BUTCHER², F. GALLAZZI², M.W. BRECHBIEL³, H. XU³, T. CLIFFORD³, T.P. QUINN², M.J. WELCH¹ and J.S. LEWIS¹

¹Radiology, Washington University School of Medicine, St. Louis, MO, USA; ²Biochemistry, University of Missouri, Columbia, MO, USA; ³Radioimmune & Inorganic Chemistry, Radiation Oncology, NCI, Bethesda, MD, USA

Introduction: Previously published work has shown that a radiolabeled rhenium-cyclized alpha-melanotropin peptide, DOTA-ReCCMSH(Arg¹¹), was successfully used to image melanoma in preclinical animal models. However, the radiolabeling procedure for the DOTA-ReCCMSH(Arg¹¹) required high temperatures and long incubation times. It was hypothesized that substitution of the macrocyclic DOTA chelator with the 5 pendent CHXA"-DTPA chelator would yield high radiolabeling efficiencies at lower reaction temperatures and shorter incubation times, facilitating formulation of the melanoma imaging agent.

Experimental: T-butyl protected CHXA" gluteric acid succinimidyl ester was coupled to the amino terminus of the CCMSH(Arg¹¹). The CHXA" conjugated peptide was cleaved from the resin, deprotected and cyclized using ReOCl₃(Me₂S)(PPh₃). CHXA"-ReCCMSH(Arg¹¹) was radiolabeled with ^{111}In , ^{68}Ga or ^{86}Y in NH₄OAc buffer at 40°C - 75°C for 20-30 min. The radiolabeled peptides were separated from free radionuclide via C18 RP-HPLC or SepPak. Biodistribution and imaging studies (PET and SPECT) were performed in B16/F1 melanoma bearing mice.

Results and Discussion: The ^{86}Y -, ^{68}Ga - and ^{111}In -CHXA"-ReCCMSH(Arg¹¹) peptides were radiolabeled at >95% radiochemical purity. In biodistribution studies, tumor uptake of ^{86}Y , ^{68}Ga and ^{111}In radiolabeled CHXA"-ReCCMSH(Arg¹¹) was 3.99 ± 0.54 , 2.46 ± 0.41 and $4.38 \pm 0.72\%$ ID/g 30 min post injection (PI), respectively, and 4.68 ± 1.02 , 2.68 ± 0.69 and $4.17 \pm 0.94\%$ ID/g 2 h PI. The tumor to blood and tumor to muscle % ID/g ratios 2 h PI for the ^{86}Y , ^{68}Ga and ^{111}In radiolabeled complexes were; 4.31 and 19.95; 4.64 and 9.69; 8.79 and 37.47 respectively. Tumor uptake of all peptides was significantly decreased 2 h post injection by co-injection with a non-radiolabeled peptide (NDP), demonstrating peptide-mediated tumor uptake of radioactivity. Clearance through the normal organs was rapid with the exception of the kidneys, which exhibited non-specific levels of radioactivity. MicroPET and microSPECT imaging of tumor bearing mice with ^{86}Y -, ^{68}Ga - and ^{111}In - radiolabeled CHXA"- ReCCMSH(Arg¹¹), with and without excess NDP blocking peptide, showed that selective tumor blocking and clear tumor visualization, respectively.

Conclusion: Radioactive dose formulation was facilitated by using CHXA"- ReCCMSH(Arg¹¹) but the lack of a chromatographic method to completely separate the radiolabeled complexes yielded lower specific activity preparations compared to their DOTA counter parts.

Acknowledgement: Grant support P50 CA103130 and R24 CA86307.

Keywords: Melanoma Imaging, CHXA"-DTPA, Y-86, Ga-68In, In-111, CHXA"-ReCCMSH(Arg¹¹)

P313 ASSESSMENT OF RADIOIODINATED BLADDER TUMOR-SPECIFIC PEPTIDE AS NON-INVASIVE DIAGNOSIS OF BLADDER TUMOR

H.Y. LEE¹, W. KWAK¹, E.-J. LEE², S.-J. OH², Y.J. LEE³, B.-H. LEE², I.-S. KIM², K.S. CHUN⁴, B.C. AHN³, J. LEE³ and J. YOO^{1,3}

¹Department of Molecular Medicine, Kyungpook National University School of Medicine, Daegu, Korea; ²Biochemistry, Kyungpook National University School of Medicine, Daegu, Korea; ³Nuclear Medicine, Kyungpook National University School of Medicine, Daegu, Korea; ⁴Korea Institute of Radiological & Medical Sciences, Seoul, Korea

Introduction: Bladder carcinoma is the most common urothelial malignancy in developed countries and the rate of recurrence is pretty high. Currently, the gold standard method in diagnosis and follow-up procedure of bladder cancer is cystoscopy, which is invasive and uncomfortable. Therefore, new non-invasive diagnosis method of bladder tumor would be very helpful.

Experimental: A 9-mer bladder tumor-specific peptide (BP), which is discovered from the phage display method, was synthesized by peptide synthesizer, and additional tyrosine was conjugated at the *N*-terminal for radioiodination (BP-Y). Another peptide, sBP-Y in which peptide sequence is scrambled, was also prepared and used as a control peptide. The two peptides were labeled with I-123 and I-124. Bladder tumor model was induced in F344 female rats by drinking water containing 0.05% BBN. For xenografted tumor model, human bladder cancer cell (HT1376) and melanoma cell were implanted on each flank in Balb/c nude mouse. Comparison microPET studies with [¹²⁴I]-BP-Y and [¹²⁴I]-sBP-Y were performed in bladder tumor-induced rats at 14 h and 37 h. For biodistribution study, the rats with induced bladder tumor were sacrificed at 4 h and 15 h after injection of [¹²³I]-BP-Y. The bladder tumor xenografted mouse was microPET imaged with [¹²⁴I]-BP-Y at 5.5 h post-injection.

Results and Discussion: The structures of two peptides were confirmed by LC/MS. The radiolabeling yield of peptides with I-123 and I-124 was over 25%, and radiochemical purity was over 90% after HPLC purification. In comparison studies between [¹²⁴I]-BP-Y and [¹²⁴I]-sBP-Y in tumor-induced rats, [¹²⁴I]-BP-Y showed higher activity uptake in bladder compared to that of [¹²⁴I]-sBP-Y at both time points. The %ID/g of bladder at 4 h is 0.29 ± 0.06 while that of muscle and liver is 0.06 ± 0.02 and 0.11 ± 0.04 , respectively. In xenografted mouse injected with [¹²⁴I]-BP-Y, bladder tumor was clearly seen in microPET images while activity uptake in melanoma was comparable with background.

Conclusion: The two peptides were synthesized successfully and radiolabeled by I-123 and I-124. MicroPET imaging and biodistribution studies clearly showed that [¹²⁴I]-BP-Y bound to bladder tumor specifically and was retained in tumor in longer period. The bladder tumor could be diagnosed non-invasively at early stage and easily screened for recurrence by using [¹²⁴I]-BP-Y.

Acknowledgement: This work was support by the Brain Korea 21 Project in 2007 and AMTC4D&P.

Keywords: Bladder Tumor, Phage Display, Disease Specific Peptide, I-124, MicroPET

P314 SYNTHESIS AND EVALUATION OF ^{18}F -LABELED PIB AS AMYLOID IMAGING AGENTS

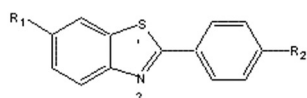
M.-Q. ZHENG, D.-Z. YIN, L. ZHANG, D.-F. CHENG, Y.-X. WANG and H.-C. CAI

Radiopharmaceutical Center, Shanghai Institute of Applied Physics, CAS, Shanghai, China

Introduction: A series of novel 6-substituted benzothiazole anilines as potential β -amyloid PET and MRI tracers were prepared. The affinities of 6 compounds for AD human brain homogenate were compared. The fluorine-18 labeled compound ^{18}F -O-FEt-PIB was selectively synthesized and its in vitro and in vivo characters were evaluated.

Experimental: The novel 6-substituted benzothiazole anilines were prepared from proper 2-amino-6-substituted benzothiazoles through base hydrolysis, intermolecular cycloaddition and N/O-alkylation reaction. The affinities were analyzed by competitive radioligand binding studies in human brain homogenate of ^3H -PIB and the K_i values are around 1nM. $60\mu\text{Ci}/200\mu\text{L}$ of ^{18}F -O-FEt-PIB was incubate at room temperature for 25min with AD and normal postmortem brain hippocampal sections for Autoradiography. In the microPET experiment, 1mCi ^{18}F -O-FEt-PIB was injected via vein to the model and control rats and 5min later scanned for 10min.

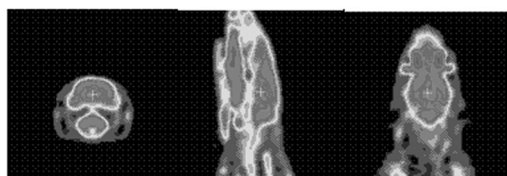
Results and Discussion: The autoradiography imagings were very different between AD brain hippocampal sections and normal's sections. The microPET in model rat brain (hippocampal in right brain was injected A β) showed the tracer existed more in the right than the left brain.



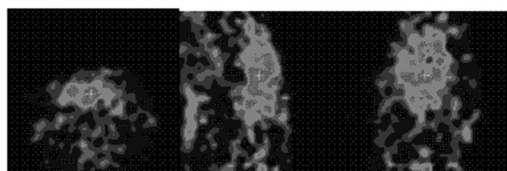
6-substituted benzothiazole aniline

 $R_1 = \text{Br}, \text{F}, \text{OH}, \text{CH}_3\text{O}, \text{FCH}_2\text{CH}_2\text{O}$ $R_2 = \text{NH}(\text{CH}_3), \text{N}(\text{CH}_3)_2$ Table 1 The values of K_i of 6-substituted benzothiazole anilines with AD brain homogenate

R_1	R_2	K_i (nmol)
	NHCH_3	$\text{N}(\text{CH}_3)_2$
F	0.20	0.31
Br	0.72	2.73
$\text{OCH}_2\text{CH}_2\text{F}$	0.17(reference)	---
OH	1.59	---



^{18}F FDG in normal rat brain, Provided by Wang Jing, Second Affiliated Hospital of Zhejiang University, China.



^{18}F O-FEt-PIB in model rat brain

Conclusion: The data suggest the potential of benzothiazole aniline derivatives as appropriate tracers for PET and MRI imaging of β -amyloid in AD brain.

Acknowledgement: The authors will thanks for Li-sheng Cai from Molecular Imaging Branch, National Institute of Mental Health, National Institutes of Health, Bethesda, MD 20892, USA and Jiang-ning Zhou from University of Science and technology. They are kindly to provide us AD human brain homogenate and AD brain sections.

Keywords: Alzheimer's Disease, β -Amyloid Plaque, Benzothiazole Aniline Derivatives, PET Ligand, MRI Tracer

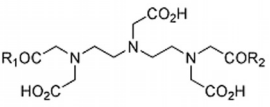
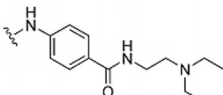
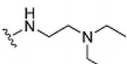
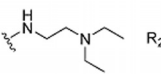
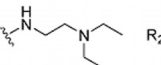
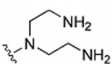
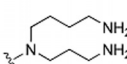
P315 POLYAMINE TRANSPORTER-MEDIATED UPTAKE OF Gd-DTPA-POLYAMINE COMPLEXES IN TUMOR CELLS: A PARADIGM FOR MRI CONTRAST AGENTS

M. WOLF¹, W.E. HULL¹, U. BAUDER-WUEST¹, D. OLTMANNS¹, U. HABERKORN², W. MIER² and M. EISENHUT¹

¹Dep. Radiopharm. Chem., DKFZ, Heidelberg, Germany; ²Dep. Nucl. Medicine, Univ. Clinics, Heidelberg, Germany

Introduction: The pharmacophore 2-(diethylamino)ethyl-carboxamide enhances the intracellular delivery of a series of technetium metal complexes in melanoma cells. High melanin affinity was also found for spermidine-substituted benzamides or the polyamines themselves. Biogenic polyamines (putrescine, spermidine, spermine) are internalized by receptor-mediated active transport processes which can result in the accumulation of up to millimolar quantities with intra-to-extracellular ratios of polyamines as high as 1000. We determined whether basic amine substituents or polyamines (Chart) are able to facilitate intracellular uptake and retention of Gd-DTPA complexes in tumor cells to serve as a MRI contrast agent (CA).

Results and Discussion: Uptake of Gd(DTPA) into cultured tumor cell lines (B16 mouse melanoma, MH3924A Morris hepatoma) was below the detection limit (ICP-MS) while CA with the melanin-binding pharmacophore 2-(diethylamino)ethylamine reached intracellular concentrations of ca. 0.03 fmol/cell (ca. 20 mM) for melanoma and 0.02 fmol/cell for hepatoma (24-h incubation with 10 mM Gd-1). With the polyamine substituents bis(2-aminoethyl)amine (Gd-3) or spermidine (Gd-6), CA uptake increased up to three-fold for melanoma (0.083 fmol/cell) and nine-fold for hepatoma (0.18 fmol/cell). Uptake of polyamine-substituted CA was reduced to ca. 15% by the polyamine transport inhibitor benzyl viologen. At 7 T molar relaxivities r_1 for three Gd-DTPA-polyamine complexes were in the range 5.6 - 6.9 for the free complex in solution, and for Morris hepatoma intracellular relaxivities were estimated to be 7.7 - 23.5 s⁻¹ mM⁻¹, based on CA uptake and R_1 measurements of cultured cell pellets. T_1 -weighted MRI at 2.35 T of rats bearing s.c. MH3924A tumors showed contrast enhancement in tumor at 1 h and 24 h post injection of 100 mmol/kg polyamine-substituted CA.

		Ligand	Gd-Complex	
				
R ₁ = R ₂	OH		DTPA	Magnevist
R ₁ = R ₂		1	Gd-1	
R ₁ = R ₂		2	Gd-2	
R ₁		3	Gd-3	
R ₁		4	Gd-4	
R ₁ = R ₂		5	Gd-5	
R ₁ = R ₂		6	Gd-6	

Conclusion: The Gd-DTPA-polyamine complexes tested exhibited suitable relaxivities in solution, predominantly transporter-mediated uptake, high intracellular relaxivities, and sufficient T_1 -weighted contrast in vivo for s.c. tumors vs. muscle. Work is in progress with alternative chelators such as DOTA. This research is a classical example that research in radiopharmaceutical chemistry can stimulate the development of new intracellular MRI imaging agents for tumor diagnosis.

Keywords: Polyamine Transporter, Gd-DTPA Complexes, MRI Contrast Agent, Tumor Imaging

P316 MicroPET IMAGING OF TUMOR PHENOTYPES USING Cu-64 AND I-124-LABELED ANTIBODY FRAGMENTS

T. OLAFSEN¹, V.E. KENANOVA¹, J.V. LEYTON¹, D. BETTING¹, A.A. RAUBITSCHKE², J.M. TIMMERMAN¹, R.E. REITER¹ and A.M. WU¹

¹David Geffen School of Medicine at UCLA, Los Angeles, CA, USA; ²City of Hope National Medical Center, Duarte, CA, USA

Introduction: PET imaging with ¹⁸F-DG is rapidly becoming commonplace in the diagnosis of patients with cancer. However, some tumors such as prostate and low-grade lymphomas are not FDG-avid and may be 'missed', 'masked' or 'mimicked' by other pathologies. A specific imaging agent directed against a cell-surface target would be extremely useful and could provide complementary information. Engineered antibody fragments are specific and exhibit rapid, high-level tumor targeting combined with fast clearance from the blood - characteristics ideal for imaging applications. Anti-CEA and anti-HER2 minibodies (80 kDa) and scFv-Fc DM (a 105 kDa fragment with H310A/H435Q Double Mutant) produce high contrast microPET images¹. Here, minibodies and scFv-Fc DM targeting CD20 (B-cell lymphoma) and prostate specific cell antigen (PSCA) have been generated and evaluated by microPET.

Experimental: The variable genes from anti-CD20 rituximab and anti-PSCA 1G8² mAb were used to make scFv fragments, fused to the IgG constant domains, to make minibodies and scFv-Fcs. The anti-CD20 minibody and scFv-Fc DM were conjugated to DOTA and labeled with Cu-64 for microPET imaging studies in C3H mice bearing 38C13-CD20⁺ xenografts. Additionally, all fragments were labeled with I-124. The anti-PSCA scFv-Fc DM was evaluated in SCID mice bearing LAPC-9 xenografts.

Results and Discussion: The anti-CD20 Cu-64 DOTA-conjugated minibody and scFv-Fc DM demonstrated specific tumor targeting with a positive tumor:negative tumor ratio of 2:1 for both fragments at 17-19 h. However, high activity accumulation was observed in liver and kidneys. By changing the radiolabel to I-124, normal tissue activities were greatly reduced, as metabolism and dehalogenation lead to clearance of the radioactivity. As a result, microPET images of I-124 anti-CD20 minibody and scFv-Fc DM showed striking localization to antigen-positive tumors with very low background in the rest of the mouse. At 21 h the tumor uptake for the minibody was 7.3(±1.7)% ID/g (n=4) and the positive:negative tumor ratio was 9:1. At 21 h post scFv-Fc DM injection, one mouse was sacrificed and showed 5.3% ID/g. At 48 h the signal in the tumors of the remaining mice (n=3) decreased to 1.4(±0.6)% ID/g. However, a tumor:blood ratio of 7:1 was obtained. At 21 h, the anti-PSCA I-124 scFv-Fc DM had tumor uptake of 3.1(±0.4) and positive tumor:background ratio of 3:1.

Conclusion: Engineered antibody fragments provide a platform for designing specific targeting and imaging agents against various tumor phenotypes.

References: [1] Kenanova, V. and A.M. Wu. *Expert Opin Drug Deliv.* **3**, 53-70 (2006). [2] Olafsen, T. *et al. J. Immunotherapy* In press.

Keywords: Tumor Surface Antigens, Engineered Antibody Fragments, MicroPET Imaging, Cu-64, I-124

P317 ASSAY DEVELOPMENT TO MONITOR SPECIFIC BINDING OF RADIOLABELED TRACERS TO PANCREATIC BETA-CELLS**P. MCQUADE, B.M. CONNOLLY, A.E. VANKO, C. SUR, S. PATEL, E.D. HOSTETLER, R.J. HARGREAVES and H.D. BURNS**

Imaging Research, Merck Research Laboratories, West Point, PA, USA

Introduction: Diabetes levels are at epidemic levels with the World Health Association estimating 217 million people are currently diagnosed worldwide, a 7 fold increase in the last 20 years (*Nat Med*, **2005**, 12; 75). Diabetes is caused by loss of beta-cell mass (BCM), therefore accurate measurement of changes in BCM would aid diagnosis and subsequent treatment of diabetic patients. However, at present there is no method available to do so, the major reason for this being that beta cells account for only around 1% of the pancreas, making detection difficult. An additional challenge is that the islets in which beta cells are found are 50-500 μm in diameter; therefore imaging would not measure BCM levels directly, but rather indicate overall change in pancreas uptake. As a result, assays would first have to be developed to assess the compounds specificity to beta cells. One such method we have developed is by taking fresh frozen cryostat sections of both human and cynomolgus monkey pancreas and using techniques analogous to immunohistochemical (IHC) staining see if autoradiography could be used to visualize individual islets.

Experimental: A commercially available murine monoclonal antibody (mAb) was chosen as our test compound as it binds specifically to insulin which is produced in beta cells (Lab Vision Corp, Fremont CA). Using standard coupling techniques the bifunctional chelator DOTA was conjugated (*Bioconj Chem*, **2001**, 12; 320) and the DOTA-mAb conjugate labeled with the positron emitting isotope Cu-64 (MDS Nordion). The unmodified, DOTA conjugated and Cu-64 labeled antibodies were then incubated with consecutive pancreatic tissue sections. The procedure was carried out using standard IHC practices and techniques with autoradiography determining the localization of the Cu-64 labeled mAb while for the non-radiolabeled species 3'3'-diaminobenzidine (DAB) was used to stain, with the images captured via a Nikon E1000 microscope.

Results and Discussion: DOTA conjugation did not appear to hamper antibody binding in either human or cynomolgus monkey pancreas tissue slices, with the same level of staining seen when compared against the unmodified antibody. Subsequent labeling with Cu-64 allowed auto-radiographic images to be obtained which clearly showed that individual islets could be positively identified. This was confirmed by overlaying Cu-64 images with adjacent tissue slices that were stained using the unmodified antibody.

Conclusion: DOTA conjugation had no effect on insulin binding and when labeled with Cu-64 autoradiography showed localization of [Cu-64]DOTA-mAb to individual islets. This demonstrates that this method can be used as a valuable tool for the development and screening of potential imaging agents for beta-cells.

Keywords: Beta-Cell, Diabetes, Antibody, Autoradiography, Cu-64

P318 AN ^{18}F -LABELED ANTISENSE OLIGONUCLEOTIDE AS AN IMAGING PROBE TO MEASURE CELLULAR RESPONSE TO RADIATION THERAPY

I.L. KOSLOWSKY¹, J.S. WILSON², D. MURRAY² and J.R. MERCER^{1,2}

¹Faculty of Pharmacy and Pharmaceutical Sciences, University of Alberta, Edmonton, AB, Canada; ²Oncology/Edmonton PET Center, Cross Cancer Institute, Edmonton, AB, Canada

Introduction: Antisense oligonucleotides (asODNs) show strong binding and high selectivity and can be constructed to recognize specific cellular targets such as gene regulated mRNA. Radiolabeled asODNs have the potential to image gene expression through specific mRNA targeting. We are investigating the preparation and radiolabeling of an asODN as a diagnostic probe relevant to radiation resistance in tumor cells. Resistance to radiation therapy is a common clinical problem in the treatment of many types of cancer. In those tumours expressing the *p53* gene, the induction of cell cycle arrest through the activation of the *p53* → *p21^{Waf1/Cip1/Sdi1}* (*p21*) pathway may be a major component of the resistance mechanism. Activation of this pathway can temporarily arrest cells at the G₁ and G₂ checkpoints of the cell cycle and is termed cell senescence. Cells deficient in *p21* undergo apoptosis (cell death) rather than senescence when subjected to DNA-damaging agents such as ionizing radiation. The use of a radiofluorinated antisense oligonucleotide to *p21* mRNA could be a valuable diagnostic probe to measure the early response to treatment using positron emission tomography (PET). In addition, the results would offer prognostic information to the clinician which may influence further treatment strategies.

Experimental: In 1997, Dollé *et al* (*J Label Comp Radiopharm* 1997; 36:319-330) first described the condensation of a monophosphorothioated oligonucleotide with [^{18}F]N-(4-fluorobenzyl)-2-bromoacetamide (1). The first step of this multiple-step procedure involves the radiolabeling of a trifluoromethanesulfonate precursor with ^{18}F [fluoride]. Therefore the remaining steps require the handling of potentially large amounts of radioactivity. Use of an automated synthesis unit (ASU) for this procedure will provide the rapid and reliable production necessary for a potential clinical tracer and will reduce the radiation dose to the researcher. Here we describe the preparation of the trifluoromethanesulfonate precursor and the synthesis of [^{18}F]N-(4-fluorobenzyl)2-bromoacetamide through automated synthesis using a modification of the TRACERlab FX_{FDG} ASU.

Results and Discussion: Labeling of an 18mer antisense oligonucleotide specific to *p21* gene produced mRNA using N-(4-fluorobenzyl)-2-bromoacetamide has been completed and preliminary studies with cell cultures shows the addition of the fluorinated prosthetic group does not inhibit the binding of the asODN to its target. Automation has permitted the rapid and efficient production of [^{18}F]N-(4-fluorobenzyl)2-bromoacetamide.

Acknowledgement: Alberta Cancer Board.

Keywords: Oligonucleotide, Automation, PET

P319 AN ANTI-p185^{HER2} scFv-Fc ANTIBODY FRAGMENT RADIOIODINATED WITH RESIDUALIZING LABELS

G. VAIDYANATHAN¹, T. OLAFSEN², A.M. WU² and M.R. ZALUTSKY¹

¹Duke University Medical Center, Durham, NC, USA; ²Molecular and Medical Pharmacology, Crump Institute of Molecular Imaging, University of California, Los Angeles, CA, USA

Introduction: The tumor uptake and retention of radioiodinated monoclonal antibodies (mAbs) and their low molecular weight fragments, which undergo extensive internalization after antigen binding, will be compromised if they were labeled using the direct radioiodination method. To investigate whether enhanced tumor retention can be achieved, an internalizing, 105 kDa recombinant anti-p185^{HER2} antibody fragment (scFv-C_H2-C_H3)₂¹ created from the humanized 4D5v8 mAb (trastuzumab, Herceptin[®]) was radioiodinated using residualizing labels ([¹²⁵I]SGMIB)² and [¹²⁵I]IB-Mal-D-GEEEEK³.

Experimental: The trastuzumab scFv-Fc was labeled with ¹²⁵I or ¹³¹I using Iodogen (IOD) and with [¹³¹I]SGMIB or [¹²⁵I]IB-Mal-D-GEEEEK. Paired-label internalization assays^{2,3} were performed *in vitro* with MCF7-HER2 cells. Biodistributions were performed in a paired-label format in mice bearing MCF7-HER2 xenografts.

Results and Discussion: Radiochemical yields of 68 ± 13% and 66 ± 17% were obtained for the conjugation of the scFv-Fc fragment with [¹²⁵I]SGMIB and [¹²⁵I]IB-Mal-D-GEEEEK, respectively. In MCF7-HER2 cells, the intracellularly trapped radioactivity from both [¹³¹I]SGMIB- and [¹²⁵I]IB-Mal-D-GEEEEK-labeled scFv-Fc fragments was substantially higher than that for the directly labeled scFv-Fc fragment (Fig. 1). From one paired-label study, the *in vivo* tumor uptake values (%ID/g) at 6, 24, and 48 h for the SGMIB-labeled scFv-Fc fragment were 2.9 ± 0.5, 2.0 ± 0.9, and 1.3 ± 0.5, respectively, compared to 2.2 ± 0.4, 0.6 ± 0.2, and 0.3 ± 0.1 for the IOD-labeled scFv-Fc fragment. In another paired label study, these values for IB- Mal-D-GEEEEK-scFv-Fc were 1.8 ± 0.6, 1.0 ± 0.2, and 0.7 ± 0.3 compared to 1.9 ± 0.4, 0.4 ± 0.02, and 0.2 ± 0.1 for IOD-scFv-Fc. The differences in the *in vivo* uptake between the directly labeled fragment and that labeled with the residualizing labels were statistically significant (*p* < 0.05) except at 6 h in the second set.

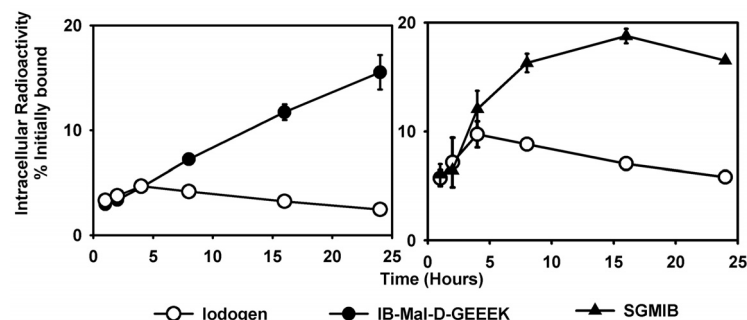


Fig. 1. Paired-label internalization of radioiodinated Herceptin scFv-Fc in MCF7-HER2 cells.

Conclusion: Taken together, the trastuzumab scFv-Fc fragment, labeled with the two residualizing labels, displayed enhanced tumor uptake and retention both *in vitro* and *in vivo*. These results demonstrate the importance of the labeling method in maximizing the potential of internalizing mAb fragments.

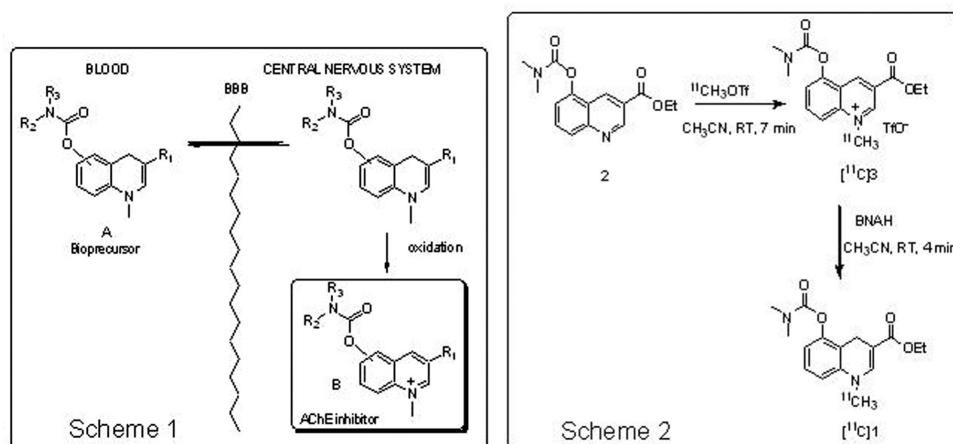
References: [1] Olafsen et al. *Cancer Res.* 2005; 65: 5907. [2] Vaidyanathan et al. *Bioconjugate Chem.* 2001; 12: 428. [3] Vaidyanathan et al. *Bioconjugate Chem.* 2006; 17: 1085.

Keywords: Herceptin, Residualizing Label, Internalization

P320 A NOVEL GENERATION RADIOTRACER FOR *IN VIVO* VISUALIZATION OF ACETYLCHOLINESTERASEF. GOURAND¹, P. BOHN², A. ABBAS¹, J. DELAMARE¹, M. DHILLY¹, M. IBAZIZENE¹, O. TIREL¹, V. LEVACHER², F. MARSAIS², D. DEBRUYNE¹ and L. BARRE¹¹GDM-TEP, UMR CEA 2E, CEA/DSV-Universite de Caen-Basse Normandie, Cyceron, Caen, France; ²Laboratoire de Chimie Organique Fine et Heterocyclique, IRCOF-INSA, Mont Saint Aignan, France

Introduction: A dysfunction of the cholinergic system, characterized by deficits in memory and cognitive functions, has been observed in several brain regions of patients suffering from Alzheimer's disease (AD). AChE inhibitors are the only class of drugs to treat AD, but these agents also exhibit peripheral cholinesterase inhibition, causing adverse side effects. To overcome this problem, a concept of bioprecursor has been envisaged to reduce the peripheral activity. This one was based on a dihydroquinoline/quaternary quinolinium ion redox system, analogous to the endogenous NADH/NAD⁺ coenzyme system. According to this strategy, the lipophilic form **A** could cross the BBB and lead after an enzymatic oxidation to the hydrophilic form **B** (Scheme 1) [1].

Results and Discussion: A series of quinolinium salts (AChE inhibitors) and their corresponding 1,4-dihydroquinolines (bioprecursors) have been synthesized.² Among them, the 3,5-disubstituted quinolinium salt **3** was evaluated *in vitro* as a potent anti-AChE inhibitor (IC₅₀=7nM). We have undertaken the radiosynthesis of the dihydroquinoline derivative [¹¹C]**1** in order to evaluate its BBB crossing and the potential of [¹¹C]**3** as a radiotracer for mapping brain AChE *in vivo* after enzymatic oxidation (Scheme 2). [¹¹C]Methyl triflate trapped at room temperature in a solution of quinoline **2** in acetonitrile afforded [¹¹C]**3**. The reduction with BNAH for 4 min led to the corresponding 1,4-dihydroquinoline [¹¹C]**1** which was injected onto a semi-preparative HPLC column. Decay corrected radiochemical yield calculated from [¹¹C]methyl triflate was 60-80% with a total synthesis time (including HPLC purification and formulation) of 55 min, the radiochemical purities greater than 99%.



Conclusion: Biological evaluation is now in progress and will be presented.

References: [1] Gourand F., Foucoute L., Levacher V., Perrio C., Debruyne D., Dupas G., Barre L., *The Quarterly Journal of Nuclear Medicine and Molecular Imaging*, **2006**, 50, 29-30. [2] Marsais F., Bohn P., Levacher V., Le Fur N., *PCT Int. Appl.*, **2006**, WO 2006103120.

Keywords: Carbon-11, Alzheimer's Disease, AChE, Bioprecursor

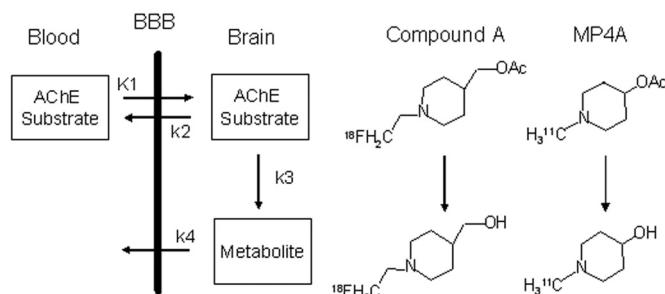
P321 EVALUATION OF THE EFFECT OF THE INCOMPLETE METABOLITE-TRAPPING ON CEREBRAL ACETYLCHOLINESTERASE ACTIVITY MEASUREMENT WITH *N*-(¹⁸F)FLUOROETHYLPYPERIDIN-4YLMETHYL ACETATE IN MONKEY PET

T. KIKUCHI, K. FUKUSHI, T. OKAMURA, K. TAKAHASHI, J. TOYOHARA, M. OKADA and T. IRIE

Molecular Imaging Center, National Institute of Radiological Sciences, Inage-ku, Chiba, Japan

Introduction: Based on metabolic trapping principle, *N*-[¹¹C]methylpiperidin-4yl acetate ([¹¹C]MP4A) has been developed and applied to measurement of decreased acetylcholinesterase (AChE) activity in the brain of patients with dementia. We have developed a ¹⁸F-labeled analogue of MP4A, *N*-[¹⁸F]fluoroethylpiperidin-4ylmethyl acetate (compound **A**). In preliminary study, the compound **A** showed high AChE specificity and moderate metabolic rate comparable to that of MP4A. However, incomplete trapping of the metabolite (k_4) was observed in monkey PET study. Here, we examined how the incomplete trapping of the metabolite affects the estimation of metabolic rate (k_3 ; an index of AChE activity).

Experimental: Using the parameter values estimated in kinetic analysis of monkey PET study and the varied k_4 ranging from 0.001 to 0.1 min⁻¹, the error-free TACs were derived. For each k_4 value, 100 different TAC data sets were generated by adding Gaussian random error to each data point of the error-free TAC. The simulation was performed with two kinetic analysis methods. One was non-linear least squares analysis with four-parameter model (FREE analysis), the other was that with fixed k_4 (three-parameter model, FIX analysis). In the FIX analysis, the alternative k_4 was applied, which was independently estimated from the later phase of TAC. From mean and standard error of k_3 estimated, precision (coefficient of variation) and bias (the difference between the estimated mean value and the true) were calculated for evaluation of the accuracy in quantitative measurement of AChE activity.



Results and Discussion: In FREE analysis, though the k_3 bias was within -3% in the entire range of k_4 , the precision became worse abruptly when k_4 is increased over 0.01. As for FIX analysis, the increase of precision was relatively gentle with increase of k_4 , while the minus bias was greater than that in FREE analysis. At 0.01 of k_4 that is close to the actual k_4 value of compound **A** in the monkey, the k_3 could be estimated with high accuracy in both analyses, and the accuracy was comparable to the case of MP4A.

Conclusion: Though the accuracy of k_3 estimate is deteriorated by incomplete trapping of the metabolite, compound **A** with rather a mild elimination of the metabolite (0.01 min⁻¹) could be applied to quantitative measurement of the cerebral AChE activity in monkey.

Keywords: Acetylcholinesterase, Positron Emission Tomography, Kinetic Analysis, Metabolic Trapping

P322 SYNTHESIS AND EVALUATION OF RS-0406 DERIVATIVES FOR BETA-AMYLOID PLAQUE AND NEUROFIBRILLARY TANGLE IMAGING

I. LEE, Y.S. CHOE, D.H. KIM, K.H. LEE, Y. CHOI, J.Y. CHOI and B.T. KIM

Nuclear Medicine, Samsung Medical Center, Sungkyunkwan University School of Medicine, Seoul, Korea

Introduction: Alzheimer's disease (AD) is pathologically characterized by the accumulation of amyloid plaques and neurofibrillary tangles in the brain. Therefore, in vivo imaging of the plaques and tangles will be useful for early diagnosis of AD. *N,N'*-Bis(3-hydroxyphenyl)pyridazine-3,6-diamine (RS-0406), a β -sheet breaker, has been known to inhibit β -amyloid (A β)(1-42) fibrillogenesis. In the present study, RS-0406 and its derivatives were synthesized and evaluated as potential ligands for A β plaque and neurofibrillary tangle imaging.

Experimental: RS-0406 was synthesized using a known method. Briefly, 3,6-dichloropyridazine (1 equiv) was reacted with 3-aminophenol (2 equiv) in 2-ethoxyethanol at 130°C for 5 h. Fluoroalkyl derivatives of RS-0406 were synthesized by reacting 3-(3-hydroxyanilino)-6-chloropyridazine (A) with 3-(fluoroalkyloxy)aniline (B) in 2-ethoxyethanol. Compound A was synthesized from 3,6-dichloropyridazine (1.2 equiv) and 3-aminophenol (1 equiv), and B was synthesized from BOC-protected 3-aminophenol and fluoroalkyl tosylate in the presence of K₂CO₃, followed by deprotection in acidic solution. Precursors for F-18 labeling were synthesized from A and 3-(bromoalkyloxy)aniline, followed by substitution of Br with tosyl group. Binding of RS-0406 derivatives to A β (1-42) aggregates was measured using [I-125]IMSB as the radiolabeled standard. Nonspecific binding was measured in the presence of 10 μ M Chrysamine G (CG). After the reaction mixture was incubated at room temperature for 3 h, the bound radioactivity to the A β aggregates was collected on Whatman GF/B filters and then counted. Data were analyzed using software Prism and K_d and K_i values were calculated.

Results and Discussion: RS-0406 and its derivatives were synthesized in overall 27-43% yields. Monofluoroalkylation of RS-0406 gave the products in low yields, and thus the derivatives were synthesized from A and B. Precursors for F-18 labeling were synthesized in overall 17-22% yields. In A β (1-42) aggregate binding assays, binding affinity of CG was also measured for a comparison with the reported value. K_i of CG (0.70 nM) was similar to the reported value (0.40 nM). RS-0406 exhibited favorable binding affinity (K_i = 15.02 nM). Of fluoroalkyl derivatives, fluoroethyl derivative showed the highest binding affinity, K_i of 0.92 nM.

Conclusion: This result demonstrates that fluoroethyl derivative of RS-0406 has high binding affinity for A β (1-42) aggregates. Preparation and in vivo evaluation of [F-18]fluoroethyl derivative of RS-0406 are currently underway.

Acknowledgement: Tributylstannyl precursor of [I-125]IMSB was a generous gift from the University of Pennsylvania. This study was supported by a grant from Ministry of Health & Welfare, Korea (A050329).

Keywords: Alzheimer's Disease, β -Amyloid Plaque, Neurofibrillary Tangle, RS-0406 Derivatives

P323 MicroPET IMAGING USING RGD-TARGETED POLY(HPMA)-DOTA-COPPER-64 CONJUGATES

F. PENG^{1,2,3}, H. ZHANG^{1,2}, H. KAUR⁴, X. LU¹, O. MUZIK^{1,2} and D. OUPICKY^{3,4}

¹Department of Pediatrics, Wayne State University, Detroit, MI, USA; ²Department of Radiology, Wayne State University, Detroit, MI, USA; ³Karmanos Cancer Institute, Wayne State University, Detroit, MI, USA; ⁴College of Pharmacological Science, Wayne State University, Detroit, MI, USA

Introduction: HPMA (*N*-(2-hydroxypropyl) methacrylamide) polymer is a biocompatible, non-toxic and water soluble polymer (1), which may be used for tumor-specific delivery of an anti-cancer drug or a therapeutic radionuclide by targeting tumor angiogenesis after conjugation of the polymer with a RGD peptide binding to $\alpha_v\beta_3$ (2,3). In this study, we synthesized and characterized a RGD-poly(HPMA)-DOTA-⁶⁴Cu conjugates, followed by microPET imaging to study their tumor-targeting capability.

Experimental: RGD-poly(HPMA)-DOTA conjugate was synthesized by aminolysis of poly(HPMA) copolymer (Mw: 40,000, containing 9.3 mol% active *p*-nitrophenyl ester) with c(RGDyK) active peptide (Peptides International, Louisville, KY) (5 mol%) and DOTA residue (10 mol%). The reaction was carried out under nitrogen in dry DMF and dry triethylamine for 20 h at room temperature. The crude conjugate was dialyzed against deionized water and lyophilized. 10-(3-aminopropyl)-1,4,7,10-tetraazacyclododecane-1,4,7-triacetic acid was used as DOTA functionality. This novel DOTA analog was synthesized from cyclen in three consecutive steps. NMR was used to characterize all intermediates and the RGD-poly(HPMA)-DOTA conjugate as well to quantify RGD and DOTA content in the conjugate. The RGD-poly(HPMA)-DOTA conjugates were radio-labeled with copper-64 and intravenously injected to the mice bearing human prostate cancer xenografts, followed by microPET imaging at 1 and 24 hour post injection (p.i.) and postmortem tissue radioactivity assay. The mice injected with copper-64 chlorides were used as control.

Results and Discussion: Nano-sized RGD-poly(HPMA)-DOTA conjugates were synthesized and characterized by NMR spectral analysis. At one hr p.i., accumulation of the RGD-poly(HPMA)-DOTA-⁶⁴Cu conjugates was clearly observed in the tumor regions, which decreased at 24 hr p.i. Tumor tissue radioactivity from the mice injected with ⁶⁴CuCl₂ was measured at 4.4 ± 0.3 ID%/g at 24 hr p.i., which was higher than that (1.5 ± 0.2 ID%/g) from the mice injected with the RGD-poly(HPMA)-DOTA-⁶⁴Cu conjugates. These findings suggested that large number of the RGD-poly(HPMA)-DOTA-⁶⁴Cu conjugates might be internalized or detached from the binding site, and eventually excreted through renal collection system by 24 hr p.i.

Conclusion: The data from this study suggested that the RGD-Poly(HPMA) polymers might be useful for targeted delivery of a therapeutic radionuclide or drug monitored by PET imaging.

Acknowledgement: The ⁶⁴CuCl₂ was provided by Washington University through an NCI/NIH grant (R24 CA86307).

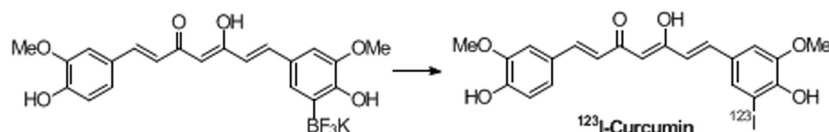
Keywords: N-(2-Hydroxypropyl) Methacrylamide (HPMA) Polymer, RGD Peptide, Angiogenesis, Positron Emission Tomography, Copper-64 Radionuclide

P324 PREPARATION AND PRELIMINARY EVALUATION OF IODINE-123 LABELED CURCUMIN, A POTENTIAL AMYLOID IMAGING AGENT

G.W. KABALKA¹, M.-L. YAO¹, B. O'NUALLAIN² and J.S. WALL²

¹ Chemistry and Radiology, University of Tennessee, Knoxville, TN, USA; ² Medicine, University of Tennessee, Knoxville, TN, USA

Introduction: Several studies on the anti-fibrillogenic and anti-oxidant effects of curcumin, a non-steroidal anti-inflammatory compound found in the spice Tumeric, have resulted in a Phase II clinical trial in patients with mild to moderate Alzheimer's disease.[1] Several studies suggest that curcumin's anti-fibrillogenic activity involves fibril-binding, destabilization and inhibition of their growth. Because of this, and the observation that curcumin inhibits amyloid fibril growth irrespective of amyloidogenic protein's primary structure, we have synthesized iodine-123 labeled curcumin and carried out preliminary binding studies using amyloid fibrils associated with non-Alzheimer's disorders, such as primary (AL) and systemic AA amyloidosis.



Experimental: The organoboron precursor was prepared using previously reported techniques.[2] The radiolabeling was carried out utilizing our recently developed boron trifluoride radiohalogenation technology.[3] Briefly, the procedure involves placing a solution of the trifluoroborate (100 μ L of 5.2×10^{-2} M solution in 50% aqueous tetrahydrofuran) in a 2 mL Wheaton vial containing no-carrier-added Na¹²³I (37 MBq in 0.1% aqueous NaOH). To this is added peracetic acid (100 μ L, 0.3% solution in methanol). The reaction vial is sealed, covered with aluminum foil, and the mixture is stirred for 10 min at room temperature. The radioiodinated product is isolated by passing it through a silica gel Sep-Pak cartridge using petroleum ether: ethyl acetate as eluent.

Results and Discussion: A radioiodinated derivative of an amyloid localizing reagent was successfully prepared using a stable trifluoroborate precursor. The results of preliminary binding studies using amyloid fibrils associated with non-Alzheimer's disorders will be presented.

Conclusion: The methodology reported is readily amenable to kit applications for the preparation of a wide variety of no-carrier-added radioiodinated amyloid imaging agents.

References: [1] <http://www.clinicaltrials.gov/ct/show/NCT00099710>. [2] Kabalka, G.W.; Mereddy, A.R. *Tetrahedron Lett.* **2004**, 45, 343-45. [3] Kabalka, G.W.; Mereddy, A.R. *Nucl. Med. Biol.* **2004**, 31, 935-938.

Acknowledgement: We wish to thank the U.S. Department of Energy, the National Institutes of Health (NCI-R01CA96128), the Robert H. Cole Foundation and the International Myeloma Foundation for support of this research.

Keywords: Radioiodination, Deboronation, Trifluoroborate, Amyloid Imaging, Curcumin

P325 AN ALTERNATIVE SYNTHESIS OF ETOMIDATE DERIVATIVES AND IN VIVO EVALUATION OF (¹²³I)IODETOMIDATE

A. SCHIRBEL¹, S. HAHNER², M.C. KREISSL¹, A. STUERMER², H. HAENSCHIED¹, M. FASSNACHT², S. JOHANSEN², I. ZOLLE³, B. ALLOLIO² and C. REINERS¹

¹Department of Nuclear Medicine, University of Wuerzburg, Wuerzburg, Germany; ²Department of Medicine, University of Wuerzburg, Wuerzburg, Germany; ³Department of Medicinal/Pharmaceutical Chemistry, University of Vienna, Vienna, Austria

Introduction: The labeled CYP11B-inhibitors [¹¹C]metomidate, [¹¹C]etomidate and [¹⁸F]fluoroetomidate are valuable tracers for adrenocortical imaging but their use is restricted to PET-centres with an on-site cyclotron. In order to extend the use of labeled derivatives of etomidate we developed [¹²³I]iodometomidate (¹²³IMTO) and evaluated this tracer in animal studies and three patients.

Experimental: The new stereoselective synthesis of iodometomidate is based on regioselective para-iodination of (R)-(+)-1-phenylethylamine followed by N-formylation, ring-closure, and oxidative desulfurization. Pharmacokinetics and biodistribution of [123/125]IMTO were studied in mice by organ distribution experiments and small animal SPECT. Three patients with different adrenocortical tumors and known or suspected metastases received 185 MBq of [¹²³I]IMTO. SPECT/CT and planar images were acquired during 28 h p.i.

Results and Discussion: Derivatives of etomidate were synthesized in high yield in gram amounts, in practice without isolating intermediates. Biodistribution experiments in mice were characterized by high tracer uptake in the adrenals and high target/non target ratios. The best results were obtained within the first hour with a maximum tracer uptake (95%ID/g) after 15 min and rapid clearance within the following 8 h. High adrenal tracer uptake and low background activity was detected with excellent visual quality by small animal SPECT. In patients, [¹²³I]IMTO displayed relative slow pharmacokinetics with a maximum tracer uptake 4-6 h p.i. Accumulation was exclusively visualized in the adrenals, all previously known adrenocortical metastases and the bladder. One suspicious bone lesion in a patient showed no uptake and later proved to be a periosteal chondroma by a subsequent biopsy. The effective radiation dose of [¹²³I]IMTO was one tenth (2.2-3.2 mSv) of the dose achieved by norcholesterol scintigraphy. An initial dosimetry with [¹³¹I]IMTO in one patient with progressive metastatic adrenocortical carcinoma showed promising results for a radiotherapy.

Conclusion: Our results demonstrate the high suitability of [¹²³I]iodometomidate for imaging of the adrenals and adrenal tumors. Furthermore we conclude that [¹³¹I]iodometomidate could be a promising radiopharmaceutical for a radiotherapy of adrenocortical carcinoma.

Acknowledgement: This work was supported by the Wilhelm Sander Foundation (grants 2003.175.1 and 2003.175.2).

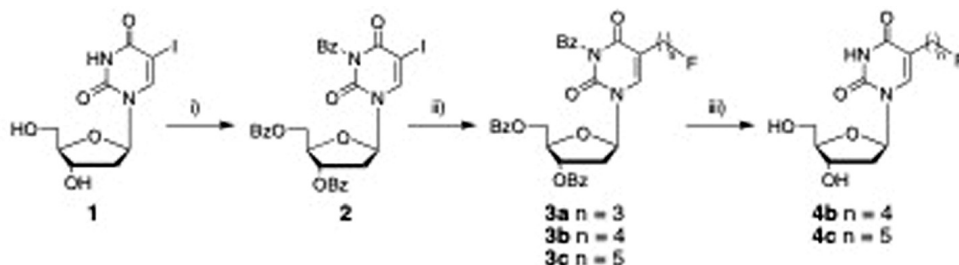
Keywords: Iodometomidate, Adrenal Scintigraphy

P326 NOVEL C-5 FLUOROALKYL NUCLEOSIDES AS HSV1-TK GENE REPORTER PROBES

A.-M. CHACKO¹, W. QU², H.F. KUNG^{1,2}, H.F. KUNG^{1,2} and A.-M. CHACKO¹Department of Pharmacology, University of Pennsylvania, Philadelphia, PA, USA; ²Department of Radiology, University of Pennsylvania, Philadelphia, PA, USA; ³Philadelphia, PA, USA

Introduction: The herpes simplex virus type-1 thymidine kinase (HSV1-tk) gene is often used as a reporter gene for the repetitive and non-invasive *in vivo* imaging of therapeutic gene expression following gene therapy. By introducing longer fluoroalkyl chains ($n \geq 3$) at the C-5 position of pyrimidine nucleosides we hope to provide easy access to improved F-18 labeled HSV1-TK protein PET reporter probes that have a much higher affinity for the viral enzyme than the analogous ceclular mammalian enzymes.

Experimental: Reported herein are the syntheses and preliminary *in vitro* findings of a novel series of C-5 fluoroalkyl nucleosides targeting HSV1-TK. The fully protected nucleosides **3b-c** were prepared by the Negishi coupling of the tribenzoyl-protected 5-iodo-2'-deoxyuridine **2** with corresponding fluoroalkylbromozinc reagents as in the described scheme. Subsequent deprotection with NaOMe afforded the final fluoroalkyl nucleosides **4b-c**. The non-radioactive nucleosides **4b-c** were initially screened as HSV1-TK probes by an *in vitro* cell uptake inhibition study with [¹²⁵I]FIAU as the reporter probe of choice in cells stably expressing HSV1-TK (RG2TK+) and control cells (RG2).



Scheme. i) Bz-Cl, DMAP, pyridine, RT, 5h; ii) BrZn(CH₂)_nF ($n = 3, 4, 5$), DMA, RT, 12h; iii) 0.5N NaOMe/MeOH, 80°C, 15min

Results and Discussion: The Negishi coupling using the key nucleoside precursor **2**, serves as a novel and rapid 2-step approach to preparing C-5 fluoroalkyl nucleosides **3b-c**. Interestingly, attempts at preparing (3-fluoropropyl)zinc(II) bromide were unsuccessful, hence **3a** could not be obtained. This coupling approach will be applied to the synthesis of precursors for F-18 labeling. The results of the *in vitro* assay suggest that the accumulation of [¹²⁵I]FIAU in RG2TK+ cells were most sensitive to FIAU (potency in the sub-micromolar range) relative to **4b-c** and ganciclovir with potencies in the low micromolar range. The relative IC₅₀ values indicate that **4b-c** have an affinity for HSV1-TK although one order of magnitude lower than FIAU.

Conclusion: In conclusion, the preliminary *in vitro* data establish that C-5 fluoroalkyl nucleosides **4b-c** do have potential as HSV1-TK PET probes. Further studies will include radiolabeling of the appropriate precursors with F-18 and *in vitro* and *in vivo* studies.

Acknowledgement: This research is supported by NIH grant EB-005242 to H.F.K.

Keywords: Nucleosides, HSV1-TK, PET, Gene Therapy

P327 DESIGN AND SYNTHESIS OF NOVEL CLASS RADIOLIGANDS FOR VISUALIZATION OF AMYLOID PLAQUE

K. HATANO¹, K. ADACHI¹, S. IWASA², M. OGAWA³, Y. MAGATA³, K. SEKIMATA¹, J. ABE¹, K. ITO¹ and T. TABIRA¹

¹National Institute for Logevity Sciences, National Center for Geriatrics and Gerontology, Obu, Aichi, Japan; ²Department of Materials Science, Toyohashi University of Technology, Toyohashi, Aichi, Japan; ³Photon Medical Research Center, Hamamatsu University School of Medicine, Hamamatsu, Shizuoka, Japan

Introduction: Formation of amyloid plaque (AP) and neurofibrillary tangle (NFT) are representative features of Alzheimer disease brain. As deposition of amyloid β protein is considered to precede NFT formation, development of imaging agents, especially PET or SPECT agents, targeting AP will be useful for early diagnosis and for monitoring disease progression. We propose a series of 3-acrylpyridine derivatives as novel class radioligands to visualize AP by PET.

Experimental: 3-(5-Methyl-furan-2-yl)-1-pyridin-3-yl-propenone (**1a**) and its *N*-oxide (**1b**) were picked up along with screening of commercially available 1100 compounds using brain sections of Alzheimer disease patients. Structurally related model compounds, 3-(4-methoxyphenyl)-1-pyridin-3-yl-propenone (**2a**) and its *N*-oxide (**2b**) were radiolabeled by *O*-[¹¹C]methylation reaction using [¹¹C]methyltriflate. Brain uptake and clearance of the each product after intravenous injection to mice was examined.

Results and Discussion: Compound [¹¹C]**2a** was obtained in good radiochemical yield (64% with decay correction) using [¹¹C]methyltriflate. Oxidative conversion of [¹¹C]**2a** to [¹¹C]**2b** could not be achieved by either peracetic acid or mCPBA. However, compound [¹¹C]**2b** was directly obtained from its desmethyl precursor in acceptable yield (31%). It is considered that *N*-oxide **2b** should be more hydrophilic than its congener **2a**. Log D value for [¹¹C]**2a** and [¹¹C]**2b** were observed 2.56 and 1.52, respectively which is consistent with this speculation. However, [¹¹C]**2b** showed higher brain uptake than that of [¹¹C]**2a**. Although the mechanism of paradoxically facilitated brain entry of pyridine *N*-oxide is not known at the present status, this chemical modification should provide new strategy for drug design.

Conclusion: Series of 3-acrylpyridines were shown to be possible candidates of AP imaging agents.

Keywords: Alzheimer Disease, Amyloid Plaque, PET

P328 DEVELOPMENT OF PET RADIOPHARMACEUTICAL TARGETING A β OLIGOMER

H. YAMAGUCHI, K. HATANO, J. ABE and K. ITO

Brain Science and Molecular Imaging, National Institute for Longevity Sciences, National Center for Geriatrics and Gerontology, Obu, Aichi, Japan

Introduction: Alzheimer's disease (AD) is one of the representative types of dementia. Although the cause of the disease is not fully understood, many lines of evidence suggest that aggregation of amyloid β protein (A β) leading to formation of senile plaque should play a crucial role in the disease progression. As formation of A β oligomers should precede their aggregation and as the oligomers are considered to be more toxic than the aggregates, non-invasive detection of A β oligomer will be a powerful strategy for early diagnosis of AD. We describe herewith development of positron-emitter labeled peptides that specifically bind A β oligomers.

Experimental: First, we selected peptide sequence with a strong intermolecular interaction with A β protein from known structural information. Next, we measured binding activity of the peptides to the A β oligomers using surface plasmon resonance (SPR). And the fluorine-18 (18F) label was introduced by using the succinimidyl fluoro benzoate (SFB) coupling reaction into these peptides.

Results and Discussion: We employed the sequence of peptide based on its binding activity to the A β oligomers using SPR. Next, the substituent was introduced by the SFB reaction based on this peptide, and 18F labeled drug was synthesized. Non-invasive imaging of A β oligomer in AD brain should be principally possible with the present achievement, however, brain delivery of the labeled peptide have to be accomplished to attain this objective. Introduction of drug delivery system (DDS) to the peptide radiopharmaceutical should be considered and verified.

Conclusion: We developed the new peptide drug for PET imaging. This drug was revealed to bind A β oligomer. Non-invasive imaging of A β oligomer in AD brain should be possible when the structural improvement of this peptidic drug were achieved.

Keywords: Alzheimer's Disease, Amyloid β Protein, Peptide, SPR, DDS

P329 THE TARGETING OF *HER-2/neu* TYROSINE KINASE EXPRESSING BREAST CANCER BY 2-^{[123]I}IODOEMODIN

J.H. PARK^{1,2}, S.W. KIM¹, M.G. HUR¹, S.D. YANG¹ and K.H. YU²

¹Radiation Application Division, Korea Atomic Energy Research Institute, Jeonggeup-si, Jeollabuk-do, Korea; ²Chemistry, Dongguk University, Seoul, Korea

Introduction: Emodin (3-methyl-1,6,8-trihydroxyanthraquinone) as a chemotherapeutic drug has antitumor activities. We showed that I-123 labelled 2-^{[123]I}iodoemodin had a potential as an imaging agent for the diagnosis of glioma related with protein kinase in the previous study. Moreover emodin has been reported to inhibit *HER-2/neu* tyrosine kinase overexpressing breast cancer cells such as MDA-MB453 and BT483. Amplification and overexpression of the *HER-2/neu* proto oncogene occur in as many as 30% of breast cancers. In this investigation, we have evaluated the cellular uptake of 2-^{[123]I}iodoemodin on breast cancer cells (MDA-MB-231 and MCF-7) which express basal levels of *HER-2/neu* tyrosine kinase.

Experimental: To a reaction vial containing 150 µl of an emodin solution in ethanol (3 mg/ml), ^{[123]I}NaI solution (1.5 GBq/100µl) was added, followed by 25 µl 0.5 M H₃PO₄, 50 µl of 32% peracetic acid and 100 µl ethanol were added and the reaction was completed in 5 min at room temperature. The reaction was quenched by adding 50 µl of sodium hydrogen sulfide (0.048 M) and 100 µl of sodium hydrogen carbonate (0.06 M), and allowed to stir for additional 10 minutes. The labelling reaction was monitored by radio-TLC. The purification and isolation of 2-^{[123]I}iodoemodin were achieved by a reversed phase HPLC. The cellular uptake of 2-^{[123]I}iodoemodin was measured on human breast cancer cells MDA-MB-231 and MCF-7 at 10 min, 30 min, 60 min and 120 min, respectively.

Results and Discussion: The radiochemical yield of the 2-^{[123]I}iodoemodin was about 80% and the its radiochemical purity was over 97% after purification. The radioactivity of the 2-^{[123]I}iodoemodin was increased in a time dependent manner for both cell lines and the maximum cellular uptake were about 1.8% for MDA-MB-231 and 1.0% for MCF-7 at 120 min.

Conclusion: 2-^{[123]I}iodoemodin is considered to be used as a *HER-2/neu* expressing breast cancer imaging agent since the the radioactivity increased in a time dependent manner. The cellular uptake of MDA-MB-231 of 2-^{[123]I}iodoemodin is 1.8 folds higher than that of MCF-7. These results suggest that 2-^{[123]I}iodoemodin could be more useful imaging agent for MDA-MB-231 than MCF-7 breast cancer. Further evaluation of the cellular uptake of 2-^{[123]I}iodoemodin is in progress with *HER-2/neu* overexpressing breast cancer cells.

Acknowledgement: This research was performed for the nuclear R&D programs funded by the Ministry of Science&Technology(MOST) of Korea.

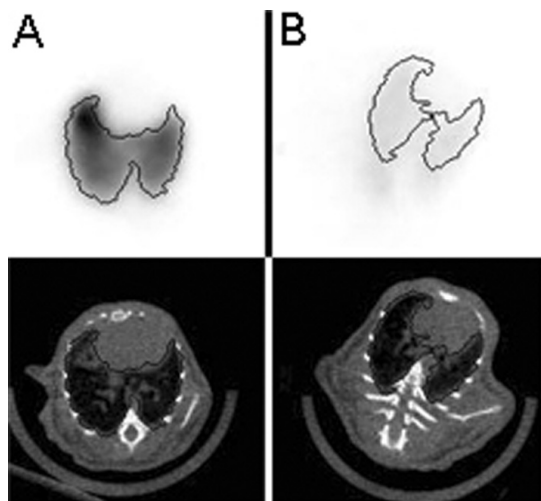
Keywords: Emodin, I-123, Breast Cancer, Imaging Agent, *HER-2/neu* Tyrosine Kinase

P330 PET IMAGING OF LUNG ENDOTHELIUM WITH ^{64}Cu -LABELED TARGETED NANOPARTICLESR. ROSSIN¹, Z. ZHOU¹, S. MURO², J. KOZLOWSKI¹, M.J. WELCH¹, V.R. MUZYKANTOV² and D.P. SCHUSTER¹¹Radiological Sciences Div., Washington University School of Medicine, St. Louis, MO, USA; ²Institute for Environmental Medicine, University of Pennsylvania, Philadelphia, PA, USA

Introduction: ICAM-1, an IgG-like glycoprotein exposed on the luminal surface of endothelial cells, is up-regulated in vascular inflammation, oxidant stress and thrombosis. For this reason, ICAM-1 is a promising target for drug delivery and lung imaging. Recently, the ability of ICAM-1 targeting nanocarriers (NCs) to reach endothelial cells and deliver a payload was confirmed both in vitro and in vivo [1,2]. Here, we have developed a method to label ICAM-1 targeting NCs with ^{64}Cu and we have investigated their use to perform lung imaging in mice with microPET.

Experimental: Control IgG was functionalized with DOTA and labeled with ^{64}Cu . Targeted and control NCs were prepared by coating polystyrene beads (100 nm) with an anti ICAM-1 monoclonal antibody or the control IgG (90% of total protein) and the ^{64}Cu -DOTA-IgG (10% of total protein). Then, the resulting NCs were pelleted, resuspended in 0.3% BSA and injected i.v. in normal C57BL/6 mice. MicroPET and microCT imaging were carried out at 1, 4, and 24h p.i. Also, at 1 and 24h p.i. mice were sacrificed (n = 2-4) and lungs and other organs of interest were harvested and counted.

Results and Discussion: The NC ^{64}Cu -labeling approach allowed the evaluation of ICAM-1 targeting in the lung in vivo by means of a small animal PET scanner. Mice administered with anti-ICAM/NCs exhibited high pulmonary activity at 1h (Figure 1A, $17.4 \pm 7.0 \mu\text{Ci}/\mu\text{l}$) which decreased to $9.8 \pm 3.5 \mu\text{Ci}/\mu\text{l}$ by 24h p.i. By contrast, low pulmonary uptake was observed when administering control NCs (Figure 1B, $3.6 \pm 1.2 \mu\text{Ci}/\mu\text{l}$ at 1h p.i.). At the same time, the mice administered with targeted beads exhibited a significantly lower accumulation in RES organs compared to controls, as confirmed by biodistribution measurements ($37.0 \pm 1.4\% \text{ID/g}$ vs $65.6 \pm 1.3\% \text{ID/g}$ at 1h p.i.).



Conclusion: These preliminary data suggest that ^{64}Cu -labeled anti-ICAM/NCs specifically accumulate in the lung endothelium by targeting ICAM-1. This strategy should allow targeted delivery to the lungs of NCs carrying therapeutic drugs which can then be monitored by PET imaging.

Acknowledgement: These experiments were supported by an NIH Program of Excellence in Nanotechnology grant (HL080729). The production of ^{64}Cu is supported by NCI grant CA86307.

References: [1] S. Muro *et al.*, *Blood*, **105**, 650-658 (2005). [2] S. Muro *et al.*, *JPET*, **317**, 1161-1169 (2006).

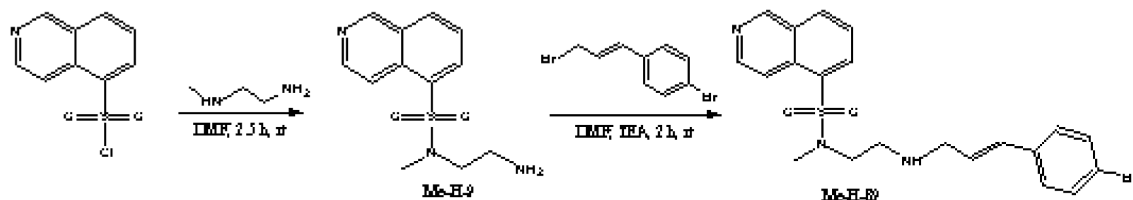
Keywords: ICAM-1, Nanoparticles, Cu-64, MicroPET, Lung Endothelium

P331 DEVELOPMENT OF (^{11}C)Me-H-89 FOR IMAGING PROTEIN KINASE AN. VASDEV¹, F.J. LARONDE², J.R. WOODGETT³, A. GARCIA¹, E.A. RUBIE³, J.H. MEYER¹, S. HOULE¹ and A.A. WILSON¹¹PET Centre, Centre for Addiction and Mental Health, Toronto, ON, Canada; ²Laro Chemicals, Toronto, ON, Canada; ³Princess Margaret Hospital, Toronto, ON, Canada

Introduction: Interventions upon cerebral protein kinase A (PKA) function are considered in the therapeutics of several neuropsychiatric illnesses, particularly in major depressive disorder based on elevations in prefrontal PKA binding after antidepressant treatment and reductions in prefrontal PKA binding in suicide victims [1]. The goal of the present study was to develop an imaging agent for measuring levels of PKA with PET.

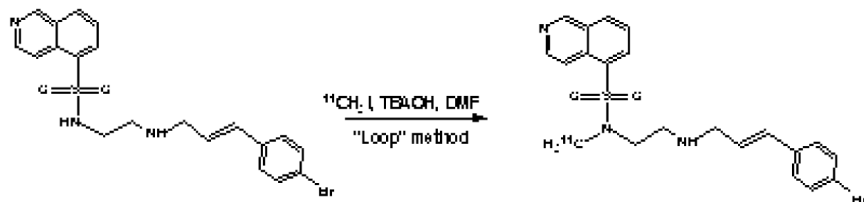
Experimental: We discovered that introduction of a methyl group to the sulphonamidic nitrogen on the PKA inhibitor *N*-[*p*-bromocinnamylamino]ethyl]-5-isoquinolinesulfonamide (H-89) does not reduce in vitro potency when tested for inhibition of PKA to phosphorylate kemptide. This promising derivative of H-89 (Me-H-89) was labelled with carbon-11 and evaluated ex vivo using rodent models.

Results and Discussion: 2-Aminoethyl-5-isoquinolinesulfonamide (H-9; precursor to H-89) and its methylated derivatives have been investigated as cardiovascular drugs [2]. We have facilitated the synthesis of Me-H-9 by reacting 5-isoquinolinesulfonyl chloride with an asymmetric diamine (20% yield; Scheme 1). Me-H-9 was thoroughly characterized by multi (^1H , ^{13}C and ^{15}N) and 2-D NMR spectroscopy, HR MS and X-ray crystallography. Me-H-9 and 1-(4-bromophenyl)-1-propen-3-yl bromide [3] were reacted to produce Me-H-89 in 16% yield (Scheme 1).



Scheme 1

H-89 was reacted with [^{11}C]CH₃I using the "Loop" method [4] (Scheme 2) to prepare [^{11}C]Me-H-89, with an uncorrected radiochemical yield of 8%, based on [^{11}C]CO₂. [^{11}C]Me-H-89 was produced ($n = 3$; 111 mCi) with >98% radiochemical purity and 1130 mCi/ μmol specific activity after 40 min. The measured log *P* was 2.93 ± 0.02 . Sprague-Dawley rats were administered [^{11}C]Me-H-89 and sacrificed at 5, 15, 30 and 60 min post-injection. Radioactivity from excised brain regions was <0.2%ID/g at all time points.



Scheme 2

Conclusion: Modest brain penetration of [^{11}C]Me-H-89 may limit its use for studying PKA in the CNS. It might still provide insight into the pharmacological mechanisms of signal transduction and a role in peripheral tumor imaging.

Acknowledgement: Funding was provided by the Canadian Society of Nuclear Medicine and GE Healthcare (NV).

References: [1] Dwivedi Y, et al. *Am J Psychiatry* 2002; **159**: 66-73. [2] Morikawa A, et al. *J Med. Chem* 1989; **32**: 42-46. [3] Hammond, ML, et al. *J Med Chem* 1990; **33**: 908-918. [4] Wilson AA, et al. *Nucl Med Biol* 2000; **27**: 529-532.

Keywords: Protein Kinase A, Carbon-11, PET, Signal Transduction, Major Depressive Disorder

P332 COMPARISON OF THE CLOCKWISE AND ANTI-CLOCKWISE STEREOISOMERS OF $(^{67}\text{Ga})\text{Ga}-(3\text{-METHOXYAL})_2\text{DMBAPEN}^{1+}$ AS MDR1 Pgp-TRANSPORT SUBSTRATES

C.J. MATHIAS, Y.-M. HSIAO and M.A. GREEN

Industrial and Physical Pharmacy, Purdue University, West Lafayette, IN, USA

Introduction: Lipophilic monocationic gallium(III) complexes of linear hexadentate salicylaldimine ligands, such as $(3\text{-MeOsal})_2\text{DMBAPEN}$ (Fig. 1), have potential utility in PET imaging of myocardium, as well as tumor imaging to assess MDR1 Pgp transport function. Chelates of this type, in which the oxygen donor atoms occupy trans-coordination sites, exhibit chirality due to the clockwise or anticlockwise arrangement of the ligand about the metal center. We report an examination of the effects of stereochemistry on chelate biodistribution in Mdr1a/b knock-out mice and FVB wild-type control animals.

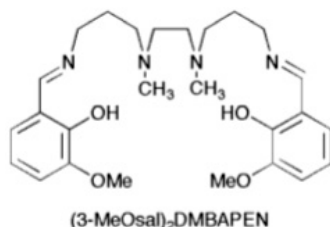


Fig. 1

Experimental: The $[^{67}\text{Ga}][\text{Ga}(3\text{-MeOsal})_2\text{DMBAPEN}]^{1+}$ was prepared by ligand exchange from $[^{67}\text{Ga}]\text{Ga}(\text{acac})_3$ in ethanol and the chelate stereoisomers were separated by HPLC using a Chiralcel OD-R column. The resolved stereoisomeric radiometal chelates were concentrated by solid-phase extraction (C18), and then recovered in ethanol for assessment of stability and biodistribution following i.v. injection.

Results and Discussion: Baseline resolution of the $[^{67}\text{Ga}][\text{Ga}(3\text{-MeOsal})_2\text{DMBAPEN}]^{1+}$ (+) and (-) stereoisomers was achieved. The resolved ^{67}Ga -chelate stereoisomers were stable, with no HPLC evidence of racemization over 8-days. Following i.v. injection, both stereoisomers were able to penetrate the blood-brain barrier of the KO-mice, but not the wild-type mice. At 1-min. post-injection, $0.99 \pm 0.11\%$ and $0.67 \pm 0.20\%$ of the injected dose was found in the brain of the KO mice for the (+) and (-) isomers, respectively, compared to $0.057 \pm 0.020\%$ and $0.047 \pm 0.015\%$ of the injected dose in the brains of the wild-type mice. Brain uptake did not substantially change with time. The clearance of this chelate from liver to bile is expected to be Pgp-mediated, but in the KO mice was also significantly affected by chelate stereochemistry. In the wild-type mice, at 1-min. the liver contained $21 \pm 6\%$ and $29 \pm 11\%$ of the injected dose for the (+) and (-) isomers, dropping to 3.2 ± 0.9 and $4.9 \pm 0.7\%$ ID at 2-hr. In the KO mice, at 1-min. the liver contained $23 \pm 4\%$ and $23 \pm 3\%$ of the injected dose of the (+) and (-) isomers. At 2-h in the KO mice, the liver uptake of the (-) isomer was essentially unchanged ($20 \pm 3\%$ of the injected dose), while the (+) isomer was partially cleared into the intestines ($7.7 \pm 2.3\%$ ID in liver), indicating the (+) isomer to have a competing, Pgp-independent, pathway for hepatobiliary excretion.

Conclusion: The biodistribution of the $[^{67}\text{Ga}][\text{Ga}(3\text{-MeOsal})_2\text{DMBAPEN}]^{1+}$ chelate is affected by Pgp expression, as well as stereochemistry about the metal center.

Acknowledgement: This work was supported by NIH Grant #RO1-CA0924403.